ISSN-1560-604X
Thermology international

Thermology International

Volume 30 (2020)
Number 4 (November)

An assessment of the role of thermal imaging of hands for its clinical usefulness in chronic hemodialysis patients.

Plantar Quad-Zone Analysis of the Feet

Employment of FLIR ONE Infrared Cameras in medicine

This journal is indexed in
EMBASE/Scopus

Published by the
European Association of Thermology

THERMOLOGY INTERNATIONAL

Volume 30(2020) **Number 4(November)**

Published by the
European Association of Thermology

Indexed in
Embase/Scopus

Organ of the American Academy of Thermology
Organ of the Brazilian Society of Thermology
Organ of the European Association of Thermology
Organ of the Polish Society of Thermology

Contents

Original article

Christopher J.Wright,Richard Collings, Jackie Morris, Ruth Clausen, Victoria Farress-Gregg
Plantar Quad-Zone Analysis of the Feet.....113
(Vier-Zonen-Analyse der Fußsohle-eine Untersuchung an den Füßen gesunder Personen

Agnieszka Gala-Bladziñska, Lech Zareba , Wojciech Marek Zylka.
An assessment of the role of thermal imaging
of hands for its clinical usefulness in chronic hemodialysis patients 121
(Eine Bewertng der klinischen Nützlichkeit der thermographischen Darstellung der Hände für chronische Hämodialyse-Patienten)

Review

Kurt Ammer
Employment of the low-cost infrared camera FLIR ONE in medicine- an overview.....128
(Der Einsatz von FLIR ONE Kameras in der Medizin-ein Überblick)

Book review

Kurt Ammer
Sonography and Thermography in the Painful Shoulder Syndrome
Review of the book "Sonografické a Termografické Nalezy Ramena" by Jozef Gabrhel.....146

Letter to the Editor

Kevin Howell
Missed reference in the article published in Thermology international 2020; 30(3) 89-90.....147

Meetings

Meetings 147

Call for abstracts for the XV Congress of the European Association of Thermology 2021.....148

Plantar Quad-Zone Analysis: A study of healthy feet

Christopher J. Wright [1], Richard Collings [2], Jackie Morris [3], Ruth Clausen[2], Victoria Farress-Gregg[2]

1 University of Exeter Medical School, Medical Imaging, St Luke's Campus, Exeter EX1 2LU, UK
2 Department of Podiatry, Torbay and South Devon NHS Foundation Trust, Castle Circus Health Centre, Torquay TQ2 5YH, UK
3 London South Bank University, School of Health & Social Care, 103 Borough Road, London SE1 0AA, UK

SUMMARY

The plantar aspect of the foot is a common site for pathology. Diabetic foot ulceration (DFU) and peripheral arterial disease (PAD) present the populations with the highest risk. Many people with diabetes experience foot neuropathy which can result in extensive skin damage. In their early subclinical phase, they are undetectable to the eye but potentially detectable using digital infra-red thermal imaging (DITI). This study aims to present a quad-zone approach to assess feet of healthy subjects for thermal symmetry and investigate the reliability of the quad-zone evaluation by multiple readers, as a precursor to clinical trials.

A FLIR T650 IR thermal camera (640x480) was used to image the soles of 30 healthy volunteers within a temperature-controlled environment. Five readers blind analysed the cases: the whole foot; and four regional zones (heel, arch, first ray, and lateral forefoot); and finally, the individual region of interest (ROI) analysis of the toes. Inter-operator reliability was assessed for the five readers. Mean values for each area of interest were assessed for contra-lateral symmetry.

Healthy feet display a wide range of temperatures: left (min=22.60, max=34.00, mean=27.57, STDEV=2.23) and right (min=22.70, max=34.10, mean=27.63, STDEV=2.32). Differences between feet or quad-zones of the same individual were consistently <1oC. Plantar toes can be significantly cooler than the rest of the foot and exhibit much greater differences (up to 2.6oC), however always <1oC between adjacent toes on the same healthy foot. No statistically significant differences between corresponding bilateral areas could be found. ICC=0.990 to 0.998 for all four quad-zones confirmed excellent inter-operator reliability in blinded assessment between five readers.

The quad zone technique is easy and time efficient to perform, ideally suited to the clinical environment, with a very high level of reproducibility. This study of feet of healthy subjects provides the underpinning evidence for further research to determine differences in the diabetic and/or neuropathic foot and seek correlation with angiographic findings.

KEYWORDS: Thermography, infra-red, DITI, thermal imaging, angiosome

VIER-ZONEN-ANALYSE DER FUSSSOHLE - EINE UNTERSUCHUNG AN DEN FÜSSEN GESUNDER PERSONEN

An der plantaren Seite des Fußes finden sich häufig krankhafte Veränderungen, am häufigsten bei Personen mit ulzerierendem diabetischem Fuß (DFU) und/oder peripherer arterieller Erkrankung (PAD). Viele Menschen mit Diabetes erfahren an den Füßen Symptome einer Neuropathie, die zu umfangreichen Hautschäden führen kann. In ihrer frühen subklinischen Phase sind sie für das Auge nicht nachweisbar, aber potenziell mit digitaler Infrarot-Thermografie (DITI) nachweisbar. Diese Studie zielt darauf ab, einen Vier-Zonen-Ansatz zur Bewertung der Füße gesunder Probanden auf thermische Symmetrie zu präsentieren und die Zuverlässigkeit der Vier-Zonen-Evaluierung durch mehrere Untersucher als Vorläuferuntersuchung für klinische Studien zu zeigen.

Eine FLIR T650 IR Wärmebildkamera (640 x 480 Pixel) wurde verwendet, um die Sohlen von 30 gesunden Probanden in einer temperaturkontrollierten Umgebung abzubilden. Fünf verblendete Untersucher analysierten die Fälle: den ganzen Fuß; und vier regionale Zonen (Ferse, Längsgewölbe, erster Strahl und seitlicher Vorfuß); und schließlich die individuell definierten Messareale (ROI) an den Zehen. Für die fünf Untersucher wurde die inter-individuelle Zuverlässigkeit bestimmt. Die Mittelwerte jedes Messareale wurden auf Symmetrie zur Gegenseite bewertet

Gesunde Füße zeigen Temperaturen über einen weiten Bereich: links (Minimaltemperatur=22.6 °C, Maximaltemperatur=34.0 °C, Mittelwert=27.6 ± 2.2 °C) und rechts (Minimaltemperatur =22.7 °C, Maximaltemperatur =34.1 °C, Mittelwert=27.6 ± 2.3 °C. Unterschiede zwischen den Füßen oder Zonen waren durchgehend kleiner als 1°C. Die plantare Seite der-Zehen kann deutlich kühler als der Rest des Fußes sein und weist große Seitenunterschiede auf (bis zu 2,6oC), die jedoch am gleichen Fuß zwischen benachbarten Zehen immer kleiner als 1oC ist. Es konnten keine statistisch signifikanten Unterschiede zwischen den entsprechenden Gebieten an beiden Seiten festgestellt werden. ICC-Werte zwischen 0.990 bis 0.998 für alle Vier-Zonen bestätigte die Zuverlässigkeit der Bewertung durch fünf geblendete Untersucher. Die Quad-Zone Technik ist einfach und zeiteffizient durchzuführen, ideal geeignet für die klinische Umgebung mit einem sehr hohen Maß an Reproduzierbarkeit. Diese Studie an Füßen gesunder Probanden liefert die Grundlage für weitere Forschungen, um Unterschiede zum diabetischen und/oder neuropathischen Fuß zu bestimmen und eine Korrelation mit angiographischen Befunden zu suchen.

SCHLÜSSELWÖRTER: Thermografie, Infrarot, DITI, Wärmebild, Vier-Zonen, Angiosom

Thermology international 2020, 30 (4) 113-120

Introduction

The plantar aspect of the foot is a common site for pathology. Diabetic foot ulceration (DFU) and peripheral arterial disease (PAD) present in populations at highest risk [1, 2]. They illustrate a significant risk factor for lower-extremity amputation and are often accompanied by a high likelihood of symptomatic cardiovascular and cerebrovascular disease. Up to 50% of patients living with diabetes experience foot neuropathy which can result in extensive skin damage, undetectable to the eye in their early subclinical phase. Up to seven thousand major lower limb amputations are performed in the UK NHS each year from complications of peripheral arterial disease and diabetes [3]. It is estimated that DFU and contingent complications cost more than £972M - 1.13Bper year [4]. An estimated 75% reduction in lower limb amputations could be possible if early preventative action were taken [5].

The standard diagnostic approach to PAD is the absence of palpable peripheral pulses and the presence of pain in the legs on walking due to claudication [6]. A more sensitive test is the ankle-brachial pulse index (ABPI), which has been validated against angiography to confirm the disease and found to be 95% sensitive and almost 100% specific. There are some limitations, however. Calcified, poorly compressible vessels in the elderly and some patients with diabetes, may artificially elevate values [7]. The ABPI may also be falsely negative in symptomatic patients with moderate aorto-iliac stenoses. Routine podiatry assessment also includes toe brachial pulse index (TBPI) and handheld Doppler signals [8].

Digital infra-red thermal imaging (DITI) is a non-invasive imaging technique that allows visualisation of the plantar foot. It has the potential to assist early diagnosis and determine thresholds of treatment protocols for all people with diabetes and PAD [9]. Areas of impending foot ulceration may manifest with localised inflammation before signs become visually apparent. This is potentially detectable by using thermal technology to show a local temperature rise of the affected skin [10]. Early research, carried out using a handheld infrared spot thermometer, suggested that the technique could be effective in the prevention of DFU [11]. A contra-lateral difference between the same area on both feet of more than 2.2°C is an indication of 'high risk' [12]. As an alternative, whole foot thermography using an infra-red thermal camera is technically easier to perform and creates a temperature map of the plantar feet. Most recent studies tend to use devices with at least 320×240 pixels, where 80% of contra-lateral differences in healthy feet fall within ±1.0 °C [13, 14, 15].

Thermal symmetry is reported between right and left feet in healthy subjects [16] and similarly between contra-lateral toes [17, 18, 19, 20]. A common approach to analysis is to use multiple regions of interest (ROI's) of approximately one-centimetre diameter, mimicking the area measured by a standard clinical infrared spot thermometer. Typically, ROI analysis is focussed around twelve plantar sites, 1st-5th toes, 1st-5th metatarsal heads, 5th metatarsal base and heel. An alternative approach to analysis is based on the principle of angiosomes; areas of skin and underlying tissue with a shared or common blood supply. The clinical relevance is well established, particularly in the surgical treatment of critical limb ischaemia, where direct revascularisation of the affected foot angiosome has been shown to improve wound healing and limb salvage rates, compared to indirect re-vascularisation techniques [21,22,23]. Four plantar foot angiosomes were originally proposed i.e. medial plantar artery (MPA), lateral plantar artery (LPA, medial calcaneal artery (MCA), and lateral calcaneal artery (LCA) [24] with the addition of a further two i.e. peroneal artery (PA) and anterior tibial artery (ATA) [25]. These anatomical territories are connected by transitional areas, creating "dynamic territories" which change with physiological status. With changes in pressure, potential vascular channels between adjoining territories either fill or lie stagnant, which means that anatomical angiosome areas and dynamic zones are often different sizes [26]. Quantitative estimation of plantar zones has been attempted using a variety of approaches [27, 28, 29, 30, 31]. A common limitation has been the analysis of only some plantar regions rather than the entire foot [32], with or without automated assessment of regions. Thermal imaging is potentially able to detect and quantify the dynamic nature of plantar zones, through repeated measurements of the same anatomical regions. A conceptual classification of twenty dynamic zones has been proposed [33] however application to clinical podiatry practice is impractical. The ability to use universally available software is desirable, as this allows for rapid dissemination throughout healthcare organisations. Analysis must be time efficient and operator independent to have clinical utility. Examination of healthy feet to establish baselines and estimation of inter-operator reliability are essential precursors to trials in clinical practice.

This research proposes to assess thermal symmetry of the plantar aspect of the foot using a novel 'quad-zone' technique based on the most common arterial pattern supplying the sole of the foot [34] and assess multi-reader reliability, as a precursor to clinical trials and future implementation.

Four regional zones (heel, arch, first ray, and lateral forefoot) are analysed, in addition to individual regions of interest (ROI's) for each toe. Any evident hot or cold spots in the thermal image are also investigated. This approach can be routinely implemented using the FLIR IR software. A study of healthy feet provides the underpinning evidence for further research involving the diabetic foot and correlation with angiographic findings.

Methods

Sample

Thirty healthy volunteers with no history of diabetes, foot ulceration, peripheral vascular disease, neuropathy, or foot

surgery were recruited by convenience quota sampling from the university population. Targeted stratification for equal ranges of age and gender occurred. All participants were provided with an information leaflet and allowed a minimum of 24 hours before giving written consent. Ethical approval was gained (Aug19/D/069Δ7), and the research was carried out in accordance with the Declaration of Helsinki.

Skin Temperature Assessment

The thermal images were recorded with an FLIR T650SC infrared camera (FLIR® Company, Wilsonville, Oregon, USA) uncooled microbolometer, 14 bit, with a high-resolution focal plane array sensor size of 640x480, noise equivalent temperature difference (NETD) of <20mK, accuracy of ±1% across the overall temperature range (calibration certificate #DN17370), and a 25° lens. Emissivity was set to 0.98.

All imaging took place within a temperature (22-24 °C) and humidity-controlled room with no windows. Ambient temperature and humidity were measured using a UMI digital monitor. Consistent with the guidelines for standardisation of thermal imaging in medicine, participants were advised not to smoke and avoid caffeinated drinks and exercise prior to the examination [35]. Upon arrival, participants removed their shoes and socks and their feet were wiped clean using a disposable towel to remove traces of debris and perspiration. They then sat on the examination couch for a 15-minute acclimatisation period with legs extended. The camera was placed on a tripod 1.5m from the plantar aspect of the participant's feet. Both feet were internally rotated 45 degrees using a standard radiographic foam pad as a guide, creating symmetry. A disposable black paper screen, with cut out sections for the ankles, was positioned to create a barrier from the participant's body and provide a surface of uniform emissivity. The foam pad acts as a positioning aid and carries a reflector from which reflected temperature (T_{REF}) can be assessed in the first stage of analysis (Figure 1).

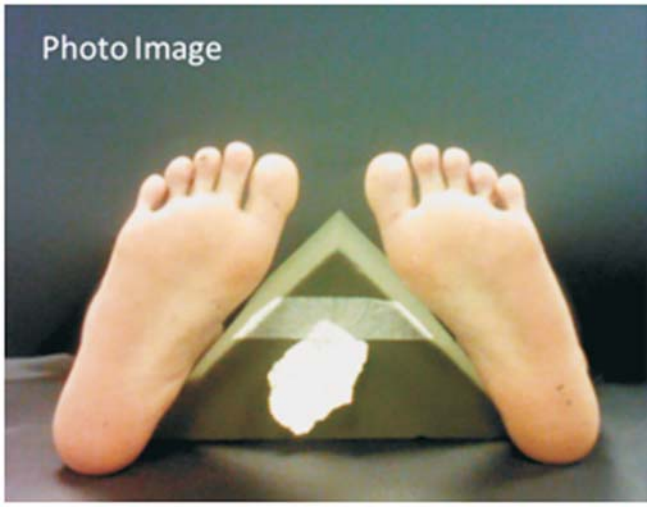

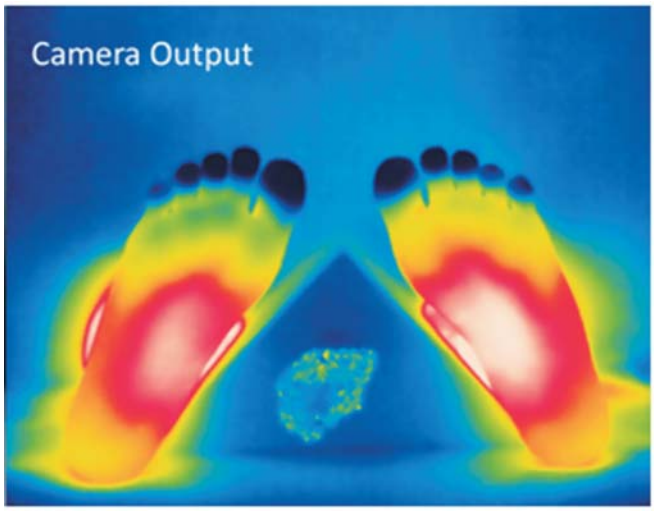

Figure 1
Corresponding photographic(left) and infra-red (right) images

Ambient temperatures (T_{AMB}) were recorded using an independent digital thermometer. Three single-shot images were acquired over three minutes in the same position to confirm repeatability.

Images were downloaded by fire-wire to the data-compiler using FLIR Researcher IR. They were then blind reported by five independent readers using a standardised technique to assess inter-operator reliability.

Analysis included:

A) **Whole foot:** Regions of interest (ROI's) drawn around the periphery of each foot.

B) **Toes:** Circular .ROI's created to fit within the boundaries of the tip of each toe (duplicated left and right).

C) **Quad Zone:** Heel, arch, first ray, lateral forefoot (see figure 2)

Figure 2
The foot divided into 'Quad-Zones'

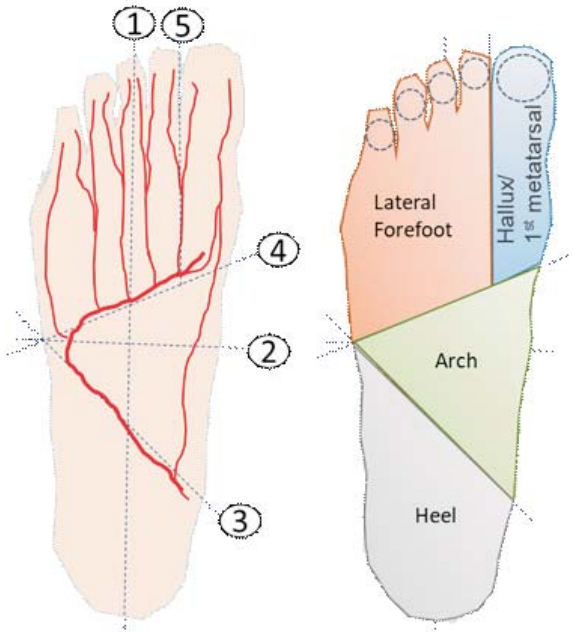

The quad zones are created by drawing:

1. A central line through the middle of the third toe to the mid-point of the heel.

2. A perpendicular bisector is drawn at the midpoint.

3. A lower intersect is drawn (40°) to follow the pathway of the lateral plantar artery

4. An upper intersect is drawn (25°) to follow the plantar arch artery.

5. A line between the first and second toes to intersect line 4 (to encompass the connection with the dorsalis pedis artery).

The size and position of each ROI are key factors [36]. Prescribing each ROI is a potential source of error, hence the need to compare the measurements of each reader for the same ROI for all feet. For toes, the potential for error is much greater due to the small size of the ROI's, and so predetermined ROI's were defined to fit within the individual toes of the sample and used by all readers.

The choice of display colour palette is a matter of personal preference. Although there are inherent limitations, a Rainbow palette is still widely used in practice [34]. This study used a "Rainbow 20" colour palette for routine image display which in some cases, made the margins of the foot, particularly toes, difficult to define, even with manipulation of level and span. Switching to a 'Sepia' colour palette for the measurement phase enabled better visualisation of margins (Figure 3).

Note how the delineated line drawn on the Rainbow image shows a small error to the medial aspect of the sole when viewed in the Sepia palette (see black ellipse). Minimum, maximum, and mean temperatures were recorded for all measurements.

Statistical analysis

Data normality was assessed using the Kolmogorov- Smirnov and Shapiro-Wilk tests. A paired-samples t-test was conducted to compare the left and right mean temperature values of the plantar foot and each of the four quad-zones

Reliability assessment considered the inter-operator agreement of the quad-zone technique via the inter-class correlation coefficient (ICC). A two-way mixed-effects, absolute agreement, average measures model was used. The standard error of measurement (SEM) was also calculated SEM=STDEV x SQRT (1 - ICC).

All statistical tests used a 95% level of significance. Statistical analyses were performed using IBM SPSS v26 statistical software package.

Results

Participant's ages ranged from 18 to 55, equally divided by gender, with shoe sizes ranging between 3.5 and 12 (United Kingdom sizing). T_{AMB} ranged from 21.4 to 24.2 °C (mean= 22.9, STDEV= 0.9). T_{REF} ranged from 22.5 to 26.1 °C (mean= 24.3,STDEV= 1.0).

The first analysis compared left and right feet using a single ROI by the five blinded readers. The mean range of these values was: Left (min 22.6°C, max 34.0 °C) and right (22.7°C, max 34.1°C). A paired-samples t-test detected no significant difference in temperature between left (mean 27.6, STDEV=2.2) and right(mean=27.6,STDEV=2.3) feet; t=-7.01, p= 0.489.

The second phase of the analysis considered the mean values of the five readers for each of the Quad zones in addition to the toes (see Tables 1 & 2).

A paired-samples t-test was conducted with 29 degrees of freedom, to compare the left and right mean temperature values of each of the four quad-zones. There was no significant difference in bilateral temperature between zones: Lateral forefoot (t=0.321, p=0.750), Hallux/1st MT (t=-0.750, p=0.941), Arch (t=2.483, p=0.210), and Heel (t=-1.765, p=0.088).

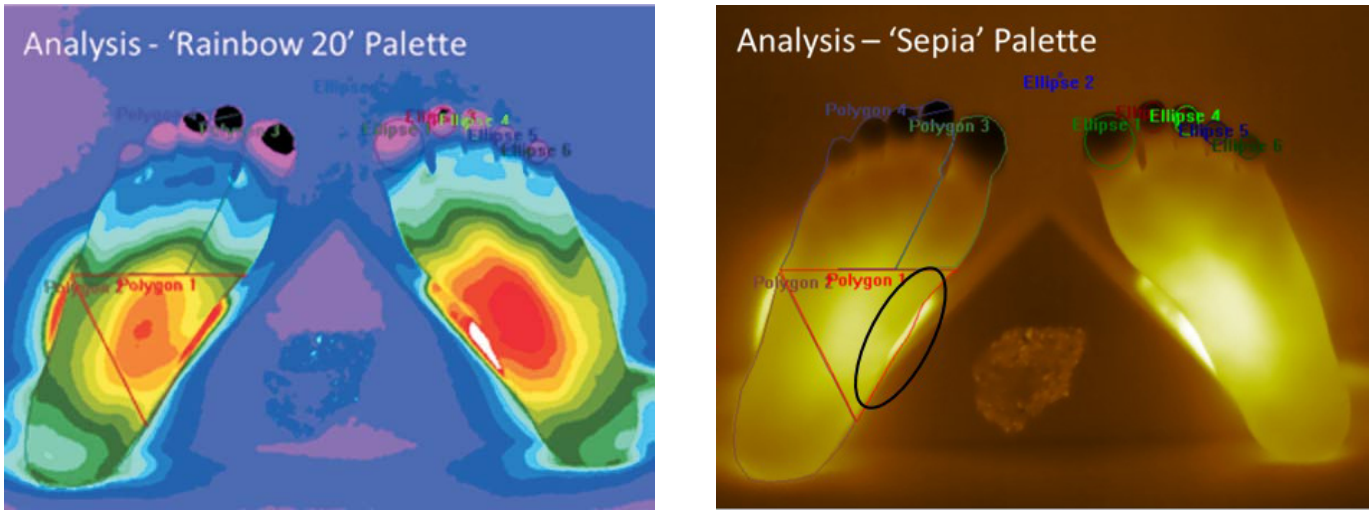

Figure 3:
Corresponding Rainbow 20 and Sepia colour palette IR images

Table 1:
Quad-Zone ROI Analysis of the feet

	Quad-Zones temperature analysis (°C)							
	Left				Right			
	Lateral forefoot	Hallux/1stMT	Arch	Heel	Lateral forefoot	Hallux/1stMT	Arch	Heel
Min	21.4	21.3	24.5	22.9	21.4	21.1	24.4	23.2
Max	34.3	34.2	34.0	33.9	34.3	34.3	34.2	34.2
Mean	27.1	27.3	28.9	27.2	27.0	27.3	28.9	27.4
STDEV	2.7	2.8	1.8	2.1	2.7	2.9	1.9	2.2
SE	1.2	1.3	0.8	1.0	1.2	1.3	0.8	1.0
95%UCL	29.4	29.7	30.4	29.1	29.4	29.8	30.6	29.4
95%LCL	24.7	28.8	27.3	25.4	24.7	24.7	27.2	25.5

Table 2
ROI analysis of the toes

	Toes temperature analysis (°C)									
	Left					Right				
	1st Toe	2nd Toe	3rd Toe	4th Toe	5th Toe	1st Toe	2nd Toe	3rd Toe	4th Toe	5th Toe
Min	19.4	18.9	19.2	19.5	19.50	19.7	19.5	19.6	19.6	19.9
Max	34.4	34.3	34.7	34.8	34.6	34.1	34.3	34.9	34.9	34.6
Mean	26.1	25.4	25.4	25.6	25.9	26.1	25.3	25.5	25.7	25.9
STDEV	3.6	3.6	3.5	3.4	3.3	3.6	3.4	3.4	3.4	3.2
SE	0.7	0.7	0.6	0.6	0.6	0.7	0.6	0.6	0.6	0.6
95%UCL	27.4	26.7	26.6	26.8	27.1	27.4	26.5	26.8	26.9	27.0
95%LCL	24.8	24.1	24.1	24.4	24.7	24.8	24.1	24.3	24.5	24.7

A paired-samples t-test was conducted with 29 degrees of freedom, to compare the left and right mean temperature values of each toe. There was no significant difference in bilateral temperature: 1st (t=0.203, p=0.841), 2nd (t=0.598, p=0.555), 3rd (t=-0.931, p=0.360), 4th (t=-0.998, p=0.332), and 5th (t=-0.079, p=0.938).

Reliability Assessment

The final phase of the analysis considers the inter-operator agreement of the quad-zone technique via the inter-class correlation coefficient (ICC). Each of the five readers drew a single ROI around each foot and the quad zone ROI's in a blinded process to create individual reports per case. The ICC is independent of the problem of a linear relationship being erroneously considered as agreement, however, is still dependent on the range of measurements. It is not related to the units of measurement or to their size [37]. In order that the ICC was not considered in isolation, the standard error of measurement (SEM) was also calculated and provides an indication of the errors that would be expected on retesting [35]. See table 3.

Discussion

The research aimed to assess the reliability of a new approach to the analysis of the plantar aspect of the foot using DITI. The findings demonstrated that healthy feet display a wide range of temperatures, 22-34°C with a mean of 27.6°C. A more valuable measurement parameter is the difference in temperature between contralateral areas on the feet.

Table 3
Inter-class correlation coefficient (ICC) and standard error of measurement (SEM)

	Left foot				Right foot			
	Average Measures	Lower 95% CI	Upper 95% CI	SEM	Average Measures	Lower 95% CI	Upper 95% CI	SEM
Whole foot	0.998	0.997	0.999	0.101	0.998	0.997	0.999	0.019
Lateral forefoot	0.994	0.989	0.997	0.206	0.995	0.992	0.997	0.192
Hallux/1stMT	0.990	0.982	0.994	0.280	0.993	0.987	0.996	0.243
Arch	0.998	0.996	0.999	0.079	0.996	0.993	0.998	0.123
Heel	0.995	0.991	0.997	0.151	0.991	0.985	0.995	0.210

Only one (n=1/30) of the healthy participants demonstrated perfect contralateral temperature for the whole feet, suggesting small differences are quite normal. As a parallel study, not yet published, two of the participants had daily foot assessment over a period of one month, highlighting how foot temperature can change by up to 10°C, yet the differences between each foot remain within a narrow bandwidth. Consistent with previous research [16, 17, 18, 19, 20], no participant had a temperature difference of >1.0°C between feet. This average measure masks the normal contra-lateral differences between quad-zones, (up to 1.3°C), which could be important in understanding the normal dynamic territory patterns of individual feet. Maximum contralateral differences between individual toes can be up to 2.6°C although, consistent with other research, the difference between adjacent toes on the same healthy foot is expected to be <1°C [20]. This highlights the importance of plotting an individual's feet to create a baseline temperature map, ideally before they become at risk of developing a foot pathology. In our experience, spot analysis, except for the toes, is difficult to reproduce. The use of the anatomical angiosome concept to define ROI's is attracting increasing interest, with unique zones for the PA, MCA, LPA, MPA [33] and ATA [38]. Whilst good levels of reproducibility have been demonstrated in a small-scale trial [39], further research is required. Moreover, question marks remain about the relevance of the anatomical angiosomes in the diseased foot where many 'dynamic territories' are created [33]. The quad zone approach, developed and tested in this study, is relatively simple and quick to perform, demonstrating very high levels of inter-operator agreement (ICC=0.990 to 0.998) in blinded analysis across five readers, and therefore has the potential to provide a valuable clinical tool. Some zonal approaches are limited to the forefoot only [40]. On the basis that the blood supply is a crucial factor in foot health, use of a zonal approach is recommended to include the whole foot in order to identify significant temperature increases when they occur, as is typical of patients with diabetic neuropathy [41, 42]. The temperature gradient from medial arch to toe might also be reversed in neuropathic feet unless masked by microangiopathy [43], which combined with an overall increase in temperature, would clearly be identified by the quad-zone technique, making it highly desirable for the assessment of patients with diabetic feet and diabetic foot ulcers. Further subdivision of the quad-zones, for example to divide the heel into Type A and Type C areas [33], is an option for additional analysis if visual difference are obvious, however unnecessary as routine.

We believe that the 'quad-zone' technique presented in this paper is a novel approach and has the great advantage of being highly reproducible with low operator dependability. Automation of the quad-zone technique offers the potential for widespread implementation in primary care and potentially in the home. With regular monitoring, it may well be possible to action proactive measures and prevent diabetic foot ulceration. New innovations are also in development, specifically designed for self-assessment by patients [44, 45] however, high resolution digital thermal imaging is likely to remain a valuable diagnostic tool in the clinical environment.

This study was limited to a single population with entry via convenience sampling. Whilst the actual temperature values recorded might not be representative of a wider population, the primary aim of the study was to test the reliability of the quad-zone technique and consider the implications for clinical practice. The quad-zone technique is limited to four ROI's which incorporate many potential dynamic zones, created due to physiological changes in the diseased foot, however, provides a useful baseline for patient assessment. Its speed and reproducibility by podiatrists as part of their routine clinical practice is paramount to knowledge transfer. Future correlation with angiographic findings involving a larger number of patients will ultimately determine the effectiveness of the technique.

Conclusion

Digital infra-red thermal imaging (DITI) combined with quad-zone analysis could be a useful technique to help determine the thresholds of treatment protocols for all people at risk of foot disease. This study of healthy feet provides the underpinning evidence for further research. The plantar foot is a common site for ulceration, particularly when linked to diabetes and peripheral vascular disease. By definition, angiosomes are limited to areas of anatomy with a common or shared blood supply, however in disease, the physiological status changes and dynamic territories are created. These changes are, in principle, visible using infra-red thermal imaging if integrated into the routine patient management protocol. Bilateral differences between healthy plantar feet, individual toes, and plantar quad-zones are expected to be <1°C, however toes are often much cooler (up to 2.6°C) than the rest of the foot.

The quad-zone technique is ideally suited to the clinical environment, being easy to perform with a very high level of reproducibility and operator independence. It would benefit from further development to include automation and artificial intelligence. Further research is on-going to determine differences in the diabetic and/or neuropathic foot and seek correlation with angiographic findings.

Declarations

a.) Ethics approval and consent to participate

Approval was gained from the University of Exeter (Aug19/D/069Δ7) and carried out in accordance with the Declaration of Helsinki. All volunteers provided written consent.

b.)Consent for publication

After reading the participant information form supported by further verbal explanation, all participants gave written consent to take part, which included the provision for their anonymised images to be used in teaching, research, and

publication. Approval for publication was granted by the Biomed central institutional membership account held by the University of Exeter Medical School. Please contact the corresponding author for data requests.

c.) Availability of data and material

Please contact author for data requests.

d.) Competing interests

The authors declare that they have no competing interests

e.) Funding

Not applicable

f.) Authors' contributions

CW acquired the images, developed the quad-zone analysis model, performed the statistical analysis, and drafted the manuscript with JM. RC, RC and VFG provided the podiatry specific content. All authors blind analysed the image case load, were involved in the editing of drafts, read and approved the final manuscript.

List of abbreviations

DFU - Diabetic foot ulcer

PAD - Peripheral artery disease

DITI - Digital infra-red thermal imaging

ROI - Region of interest

ABPI - Ankle brachial pulse index

TBPI -Toe brachial pulse index

MT - Metatarsal

T_{AMB} - Ambient temperature

T_{REF} - Reflected temperature

STDEV - Standard deviation

SQRT - Square root

ICC - Inter-class correlation

CI - Confidence interval

SEM - Standard error of measurement

References

1. Jude EB, Oyibo SO, Chalmers N, Boulton AJ. Peripheral arterial disease in diabetic and nondiabetic patients: a comparison of severity and outcome. Diabetes Care 2001; 24: 1433-1437.

2. Brownrigg JRW, Apelqvist J, Bakker K, Schaper NC, Hinchliffe RJ. Evidence-based Management of PAD & the Diabetic Foot. Eur J Vasc Endovasc Surg 2013; 45: 673-681.

3. Public Health England. Diabetes. Available at https://fingertips.phe.org.uk/profile/diabetes-ft last accessed 28th September 2020

4. Kerr M, Barron E, Chadwick P, Evans T, Kong W, Rayman G, Sutton-Smith M, Tood G, Young B, Jeffcoate W. The cost of diabetic foot ulcers and amputations to the National Health Service in England. Diabetic Medicine 2019;

5. Bus SA., van Netten JJ., et al., A shift in priority in diabetic foot care and research: 75% of foot ulcers are preventable. Diabetes/Metabolism Research and Reviews. 2016. 32(S1). 195-200

6. Khan NA, Rahim SA, Anand SS, Simel DL, Panju A. Does the clinical examination predict lower extremity peripheral arterial disease? In: Database of Abstracts of Reviews of Effects (DARE): Quality-assessed Reviews [Internet]. York (UK): Centre for Reviews and Dissemination (UK); 2006. Available from: https://www.ncbi.nlm.nih.gov/books/NBK73413/.

7. Mozos I, Malainer C, Horbaczuk J, Gug C, Stoian D, Luca CT, Atanasov AG. Inflammatory markers for arterial stiffness in cardiovascular diseases. Frontiers in Immunology. 2017; 8: 1058.

8. Nicolaï SP, Kruidenier LM, Rouwet EV, Wetzels-Gulpers L, Rozeman CA, Prins MH, Teijink JA. Pocket Doppler and vascular laboratory equipment yield comparable results for ankle brachial index measurement. BMC cardiovascular disorders. 2008; 8(1): 26.

9. Gauci J, Falzon O, Formosa C, Gatt A, Ellul C, Mizzi S et al. Automated Region Extraction from Thermal Images for Peripheral Vascular Disease Monitoring. Journal of Healthcare Engineering. 2018; 1-14.

10. Bergtholdt HT, Brand PW. Thermography: an aid in the management of insensitive feet and stumps. Arch Phys Med Rehabil 1975; 56: 205-209

11. Armstrong DG, Holtz-Neiderer K, Wendel C, Mohler MJ, Kimbriel HR, Lavery LA. Skin temperature monitoring reduces the risk for diabetic foot ulceration in high-risk patients. Am. J. Med. 2007; 120: 1042-1046

12. Armstrong DG, Lavery LA. Monitoring healing of acute Charcot's arthropathy with infrared dermal thermometry. J Rehabil Res Dev 1997; 34: 317

13. Bagavathiappan S, Philip J, Jayakumar T, Raj B, Rao P N S, Varalakshmi M, Mohan V. Correlation between plantar foot temperature and diabetic neuropathy: a case study by using an infrared thermal imaging technique. J. Diabetes Sci Technol 2010; 4: 1386-1392

14. Bharara M, Schoess J and Armstrong D G Coming events cast their shadows before: detecting inflammation in the acute diabetic foot and the foot in remission Diabetes Metab Res Rev 2012; 28: 15-20

15. van Netten JJ, van Baal JG, Liu C, van Der Heijden F, Bus SA. Infrared thermal imaging for automated detection of diabetic foot complications. J. Diabetes Sci Technol 2013; 7: 1122-1129

16. Vardasca R, Ring EFJ, Plassmann P, Jones CD. Thermal symmetry of the upper and lower extremities in healthy subjects Thermol. Int. 2012; 22: 53-60

17. Uematsu S, Edwin DH, Jankel WR, Kozikowski J, Trattner M. Quantification of thermal asymmetry: part 1: normal values and reproducibility J. Neurosurg. 1988; 69 552-555

18. Niu HH, Lui PW, Hu JS, Ting CK, Yin YC, Lo YL, Liu L, Lee TY. Thermal symmetry of skin temperature: normative data of normal subjects in Taiwan Chin Med J. 2001; 64: 459-468

19. Gatt A, Formosa C, Cassar K, Camilleri K P, De Raffaele C, Mizzi A, Azzopardi C, Mizzi S, Falzon O, Cristina S, Chockalingam N. Thermographic patterns of the upper and lower limbs: baseline data. Int. J. Vasc. Med. 2015; 831369

20. MacDonald A, Petrova N, Whittam A. Thermal symmetry of healthy feet: A precursor to a thermal study of diabetic feet prior to skin breakdown. Physiological Measurement 2016; 38: 333-344.

21. Bosanquet DC, Glasbey JCD, Williams IM, Twine CP. Systematic Review and Meta-analysis of Direct Versus Indirect Angiosomal Revascularisation of Infrapopliteal Arteries. European Journal of Vascular and Endovascular Surgery 2014; 48 (1): 88-97

22. Biancari F, Juvonen T. Angiosome-targeted Lower Limb Revascularization for Ischemic Foot Wounds: Systematic Review and Meta-analysis. European Journal of Vascular and Endovascular Surgery 2014; 47 (5): 517-522.

23. Jongsma H, Bekken JA, Akkersdijk GP, Hoeks SE, Verhagen HJ, Fioole B Angiosome-directed revascularization in patients with critical limb ischemia. Journal of Vascular Surgery 2017; 65(4):1208-1219.

24. Attinger C, Cooper P, Bulme P. Vascular anatomy of the foot and ankle. Operative Techniques in Plastic and Reconstructive Surgery 1997, 4(4) 183-198

25. Taylor G, Palmer J. The vascular territories (angiosomes) of the body: experimental study and clinical applications. British Journal of Plastic Surgery 1987; 40: 113-141

26. McGregor IA, Morgan G: Axial and random pattern flaps. Br J Plast Surg 1973; 26: 202-213.

27. Peregrina-Barreto H, Morales-Hernandez LA, Rangel-Magdaleno JJ, Avina-Cervantes JG, Ramirez-Cortes JM, Morales-Caporal R. Quantitative estimation of temperature variations in plantar angiosomes: a study case for diabetic foot. Comput Math Methods Med. 2014; 585306

28. Mori T, Nagase T, Takehara K, Oe M, Ohashi Y, Amemiya A, et al. Morphological pattern classification system for plantar thermography of patients with diabetes. J Diabetes Sci Technol. 2013; 7(5): 1102-1112

29. Clemens MW, Attinger CE. Angiosomes and wound care in the diabetic foot. Foot Ankle Clin. 2010; 15(3): 439-464

30. Peregrina-Barreto H, Morales-Hernandez LA, Rangel-Magdaleno JJ, Pd V-R. Thermal image processing for quantitative determination of temperature variations in plantar angiosomes. IEEE International.Conference on Instrumentation and Measurement Technology (I2MTC) 2013, IEEE 2013. pp. 816-820

31. Hernandez-Contreras D, Peregrina-Barreto H, Rangel-Magdaleno J, Gonzalez-Bernal JA, Altamirano-Robles L. A quantitative index for classification of plantar thermal changes in the diabetic foot. Infrared Phys Technol. 2017; 81: 242-249

32. van Netten JJ, Prijs M; van Baal JG, Liu C, van der Heijden F, Sicco A. Diagnostic values for skin temperature assessment to detect diabetes-related foot complications Diab. Technol. Therapeut 2014; 16: 714-721

33. Nagase T, Sanada H, Takehara K, Oe M, Iizaka S, Ohashi Y, Oba M, Kadowaki T, Nakagami G. Variations of plantar thermographic patterns in normal controls and non-ulcer diabetic patients: novel classification using angiosome concept, . Journal of Plastic Reconstructive & Aesthetic Surgery.2014; 64: 860-866.

34. Ring EFJ; Ammer K. The Technique of Infra-red Imaging in Medicine. . Thermology international 2000; 10. 7-14.

35. Seixas, A. Reliability: What is it, how is it determined and is it necessary for thermal imaging? Thermology international 2018; 28 (4), 187-191

36. Borland D, Taylor MR 2nd. Rainbow color map (still) considered harmful. IEEE Comput Graph Appl. 2007; 27(2): 14-7

37. Bland J,. Altman,D. A note on the use of the intra-class correlation coefficient in the evaluation of agreement between two methods of measurement. Computers in Biology and Medicine 1990; 20(5), 337-340.

38. Alexandrescu VA, Triffaux F. Ischemic Ulcer Healing: Does Appropriate Flow Reconstruction Stand for All That We Need? Wound Healing-New insights into Ancient Challenges. InTec 2016; 247-277

39. Seixas A, Azevedo J, Pimenta I, Ammer K, Carvalho R, Vilas-Boas JP, Mendes J, Vardasca R. Skin temperature of the foot: Reliability of infrared image analysis based in the angiosome concept. Infra-red Physics & Technology 2018; 92: 402-408

40. Yavuz M, Ersen A, Lavery L, Wukich D, Hirschman G, Armstrong D, Quiben M, Adams L. J Am Podiatr Med Assoc 2019; 109(5): 345-350,

41. Sun PC, Lin HD, Jao SH et al: Relationship of skin temperature to sympathetic dysfunction in diabetic at risk feet. Diabetes Res Clin Pract 2006; 73: 41,

42. Yavus M, Brem RW, Glaros AG et al. Association between plantar temperatures and tri-axial stresses in individuals with diabetes. Diabetes Care 2015; 38(10): e178,

43. Adhil Ahamed Yameen K. Reconstruction in revascularised diabetic foot. Masters thesis, Madras Medical College, Chennai. 2014. Available at: http://repository-tnmgrmu.ac.in /3499/1/180300114adhilahamedyameen.pdf

44. Najafi B, Reeves ND, Armstrong DG. Leveraging smart technologies to improve the management of diabetic foot ulcers and extend ulcer-free days in remission. Diabetes Metabolism research & reviews. 2020; e3239

45. Frykberg RG, Gordon IL, Reyzelman AM, Cazzell SM, Fitzgerald RH, Rothenberg GM, et al. Feasibility and Efficacy of a Smart Mat Technology to Predict Development of Diabetic Plantar Ulcers.. Diabetes Care. 2017; 40(7):973-80

Address for Correspondence

Christopher J. Wright

University of Exeter Medical School,
Medical Imaging, St Luke's Campus,
Exeter EX1 2LU, United Kingdom

email: c.j.wright@exeter.ac.uk

(Received. 03-08-2020, revision accepted 07-11-2020)

An assessment of the clinical usefulness of thermal imaging of hands in chronic hemodialysis patients

Agnieszka Gala-Bladzinska[1,2], Lech Zareba[3] , Wojciech Marek Zylka[4,5]

[1]Department of Internal Medicine, Nephrology & Endocrinology, St. Queen Jadwiga Clinical District Hospital No.2 , Rzeszow, Poland
[2] Medical College of Rzeszow University, Institute of Medical Sciences, Rzeszów, Poland
[3] Interdisciplinary Centre for Computational Modelling, College of Natural Sciences University of Rzeszów, Rzeszów, Poland
[4] The Didactic Centre of Technical and Natural Sciences , College of Natural Sciences, University of Rzeszow, Rzeszow, Poland
[5] Department of Electronics, Telecommunications & Mechatronics, Polytechnic Faculty, University of Applied Sciences, Tarnów, Poland

SUMMARY

PURPOSE: The aim of this study was to assess the potential of thermal imaging of the hands of patients undergoing hemodialysis due to end stage renal disease as a risk marker for cardiovascular events and/or mortality.

METHODS: At start, we examined skin temperature of patients' hands using a thermal imaging camera; measuring both hands at the fingertips and wrists with, and without arteriovenous fistula (AVF) and above the AVF. Combined with thermal imaging, blood sample results used routinely for monitoring haemodialysis were recorded. During a follow period of 48 months, incident cardiovascular events and deaths were recorded. We correlated temperatures with blood sample results, concomitant diseases, and cardiovascular complications.

RESULTS: The study included 34 (13 women; 38.2%) chronically haemodialysed adult patients with an average age of 64.74 ± 15.29 years, with AVF (n = 24; 70.6%) or catheter. Hand temperature measurements were not significantly different in respect to sex, cardiovascular disease, stroke, lower limb amputation or death ($p > 0.05$). Serum albumin concentrations had a significant effect on the average temperature of fingertips without AVF in the entire study population ($p = 0.01$; $R = - 0.40$). In patients haemodialyzed with AVF compared to those dialysed with a catheter, we observed significantly lower temperatures in the fingertips of both hands ($p < 0.05$) and in AVF fingertips ($p = 0.03$) regardless of other clinical and laboratory data tested. Haemodialysis patients with a catheter had significantly ($p < 0.05$) lower body weight, higher calcium-phosphate index, higher CRP, lower serum albumin and higher ear canal temperature than patients dialysed with AVF.

CONCLUSION: In our study we have shown that thermal imaging of hands can be clinically useful, and is a non-invasive method for assessing malnutrition-inflammation- atherosclerosis syndrome. Furthermore, low acral temperatures might indicate subclinical ischemia in the fingertips of patients with AVF.

KEYWORDS: thermal imaging; hemodialysis; malnutrition-inflammation-atherosclerosis syndrome

EINE BEWERTUNG DER KLINISCHEN NÜTZLICHKEIT DER THERMOGRAFISCHEN DARSTELLUNG DER HÄNDE FÜR CHRONISCHE HÄMODIALYSE-PATIENTEN

ZWECK: Ziel dieser Studie war es, das Potenzial der Thermografie der Hände von Patienten, die sich aufgrund einer Nierenerkrankung im Endstadium einer Hämodialyse unterziehen, als Risikomarker für kardiovaskuläre Ereignisse und/oder Mortalität zu bewerten.

METHODEN: Zuerst erhoben wir mit einer Wärmebildkamera die Hauttemperatur an den Fingerspitzen beider Hände, am Handgelenk mit und der Seite ohne arteriovenöse Fistel (AVF) als über der AVF. Gleichzeitig mit den Wärmebilddern wurden die routinemäßig zur Überwachung der Hämodialyse verwendeten Blutproben aufgezeichnet. Während eines Folgezeitraums von 48 Monaten wurden kardiovaskuläre Ereignisse und Todesfälle registriert. Wir korrelierten die Temperaturwerte mit Blutprobenergebnissen,den Begleiterkrankungen und Herz-Kreislauf- Komplikationen.

ERGEBNISSE: Die Studie umfasste 34 (13 Frauen; 38,2 %) chronisch-dialysierte erwachsene Patienten mit einem Durchschnittsalter von 64,74 ± 15,29 Jahren, mit AVF (n = 24; 70,6%) oder Katheter. Die Handtemperaturmessungen unterschieden sich nicht signifikant in Bezug auf Geschlecht, Herz-Kreislauf-Erkrankungen, Schlaganfall, Amputation der unteren Gliedmaßen oder Tod ($p > 0,05$). In der gesamten Studienpopulation ohne AVF war die Serumalbuminkonzentration signifikant mit der durchschnittlichen Temperatur der Fingerspitzen korreliert ($p = 0,01$; $R = - 0,40$). Unabhängig von anderen klinischen und Labordaten beobachteten wir bei Patienten, die mit AVF im Vergleich zu Patienten mit einem Katheter hämodialysiert wurden, signifikant niedrigere Temperaturen an den Fingerspitzen beider Hände ($p < 0,05$) und an den Fingerspitzen der AVF-Seite ($p = 0,03$). Mit einem Katheter dialysierte Patienten hatten ein signifikant ($p < 0,05$) geringeres Körpergewicht, einen höheren Calcium-Phosphat-Index, ein höheres CRP, ein niedrigeres Serumalbumin und höhere Gehörgangtemperatur als Patienten, die mit AVF dialysiert worden waren.

SCHLUSSFOLGERUNG: In unserer Studie haben wir gezeigt, dass die thermografische Darstellung der Hände klinisch nützlich sein können, und als nicht-invasive Methode zur Beurteilung von Unterernährung- Entzündung-Arterio- sklerose- Syndrom dienen können. Darüber hinaus könnten niedrige akrale Temperaturen auf eine subklinische Ischämie in den Fingerspitzen von Patienten mit AVF hinweisen.

SCHLÜSSELWÖRTER: Thermografie; Hämodialyse; Mangelernährung-Entzündung-Atherosklerose-Syndrom

Thermology international 2020, 30(4) 121-127

Introduction

Because the human body is emitting infrared radiation from the surface, the human organism is perfectly suited to thermal imaging. Visualizations of temperature patterns on the body can be diagnostically useful, because the surface temperature may reflect of internal physiological and pathological processes [1-3]. Research into military applications for infrared detectors carried out during the Second World War stimulated a rapid development of thermography. The medical use of thermography was initiated by Ray Lawson in 1956, where his early studies were focused on breast cancer [3]. Today, thermography is used as a complementary diagnostic tool in various disorders such as Raynaud's syndrome [4], arthritis [5], and several others [6]. It was also used used as an outcome measure in trials with anti-inflammatory drug, physical therapy and surgical interventions [7].

Infrared radiation is a form of electromagnetic radiation; other familiar forms of electromagnetic radiation are visible light and radio waves. Infrared wavelengths range between 0.78 and 1000 μm; they are longer than visible light waves, but shorter than radio waves. They are classified from near infrared to far infrared. Electromagnetic radiation is produced by the movement of atoms and molecules on the surface of an object when the object's temperature is higher than absolute zero. Certain electromagnetic waves are capable of transporting quantities of thermal energy with wavelengths between 2 und 30μm representing infrared thermal radiation. A thermographic camera captures the emitted infrared radiation, transforming the radiated energy into electricity and further to temperature, creating in that way a gray-shade image representing the temperature distribution on the surface of the objects studied, including on the surfaces of the human body.

There are several reasons why the application of thermal imaging in the diagnosis of certain disorders is advantageous. First, due to thermal imaging the distribution of temperature on the surface of an object, also on human body, can be visualized and recorded. Second, since thermal imaging is a fast, non-contact, non-invasive method, it can be conducted directly at the patient's bedside. Furthermore, staff performing the procedure can be trained relatively quickly, with the results (i.e. temperatures measured) being easy to interpret, and the procedure being easy to repeated. The thermo- grams obtained can be processed and analyzed on a computer [12,13]. Thermal imaging has been applied in monitoring of dialysis patients. Austrian [8], British [1,9], and Polish [10,11,] researchers have shown that the state of arteriovenous fistulas can be effectively and easily monitored by the non-invasive technique of thermography. In the available literature we have not found any studies correlating the results of thermovision studies with cardiovascular complications and biomarkers of chronic hemodialysis. It is known that in the population of chronically haemo- dialysed patients, chronic inflammation associated with uremia, coexisting diseases, repeated blood extravasation during haemodialyses, blood clotting within haemodialysis drains that persist on the dialyser surface, which may promote cardiovascular complications and increase the mortality in this group of patients [14,15]. However, it not yet established that infrared thermal imaging can serve as a valid riskfactor of cardiovascular complications or can be used for assessment of well-being of chronically haemo- dialysed patients The aim of this study was to assess the the potential of thermal imaging of the hands of patients undergoing hemodialysis due to end stage renal disease as a risk marker for cardiovascular events and/or mortality.

Materials and Methods

The tests have been performed in dialysis center with 10 dialysis stations, operating in a regional hospital with approximately 1,000 beds. The study was conducted in August 2015. The clinical follow-up period for the study group was 4 years (from August, 2015 to August 31, 2019). Before taking part in the study, all participants gave their voluntary, informed consent. The study was conducted in accordance with the Declaration of Helsinki and with the consent of local Bioethics Committee.

A thermal imaging camera was used to register the thermal field of the skin surface in chronic hemodialysis patients, as well as to measure the temperature of their hands. The hand skin temperature was measured with the NEC Avio Infrared R300 Thermal Imaging Camera (NEC Avio Infrared Technologies Co., Ltd.). The R300 NEC camera has a detector with a resolution of 320x240 pixels and an uncooled microbolometer matrix made in modern technology. The field of view of the recorder with a standard lens is 22 ° x17 °. The device is equipped with a continuous digital zoom from x1 to x4. The declared thermal resolution of the matrix (NETD) is 0.03 ° C (at 30 ° C), the accuracy is ± 1 ° C, and the spatial resolution or the instantaneous angle of view (I.F.O.V) is 1.2 mrad. Emissivity was 1.0.

In order to eliminate any negative influence of low ambient temperatures, the temperature of the hands was measured directly before the patient's dialysis session, in a separated examination room, when the external temperature was 28 °C and the examination room temperature was from 25.0 to 26.7 °C. The patients acclimated for to the room temperature of about 15 minutes. Patients were asked to put both their hands on a sheet of paper, used only once, which was laid on the examination table. Thermo- grams were recorded by the same person, in accordance with a previously prepared repeatable standard. Appropriate rules have been set out, the areas in which the measurement was carried out. These areas were agreed with dialysis specialists - previously discussed and carefully selected. e.g. fingertips, etc. In each patient, one point of temperature measurements was performed in the determined test area marked in Figure 1. Received results of temperature measurements were taken and the value was given as an average. In the whole group of patients, temperature measurements were taken

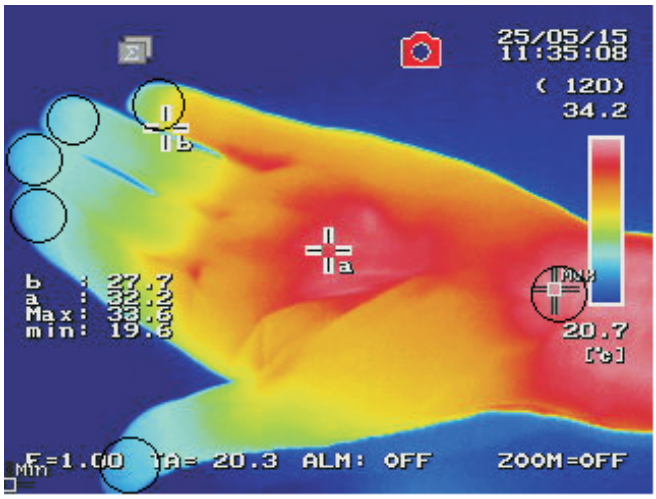

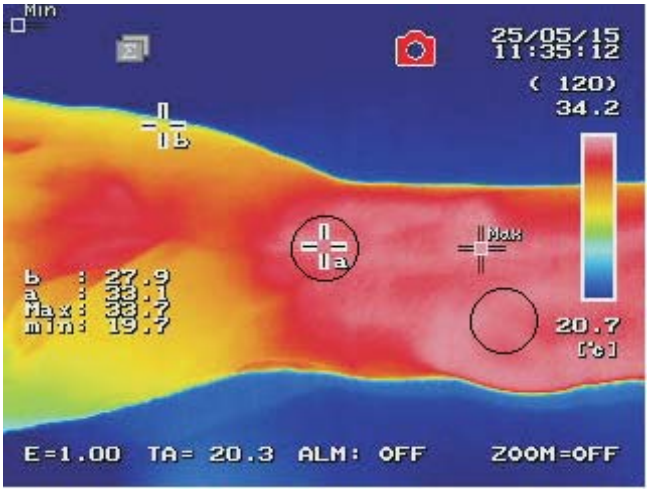

Figure 1.
Measurement areas

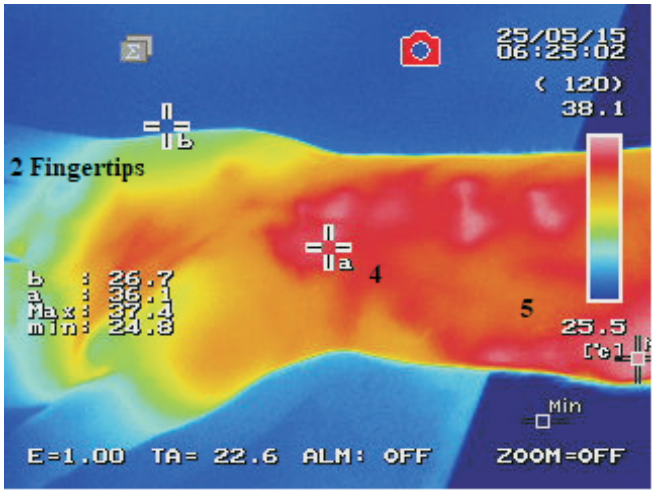

Figure 2a.
Temperature measurements on the upper limb with an arteriovenous fistula (all hemodialysed patients using arteriovenous fistula had an arteriovenous fistula in the left wrist or left forearm)

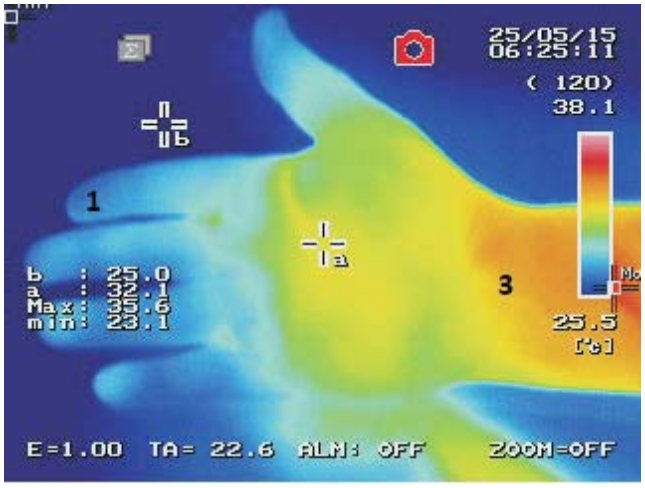

Figure 2b
Ttemperature measurements on the upper limb without an arteriovenous fistula
1. The fingertips of the upper limb without an arteriovenous fistula (always right hand).
2.The fingertips of the upper limb with an arteriovenous fistula.
3. Wrist without arteriovenous fistula.
4. Wrist with arteriovenous fistula.
5. Arteriovenous fistula.

on the fingertips and on the wrist of both hands. Special attention was paid to the distinction between dialysis patients using a catheter and patients using an arteriovenous fistula (AVF). In addition, the AVF surface temperature was measured in AVF patients. The places on the hand where temperature measurements were taken are indicated in Figure 2. From the arithmetic sums of the hand temperatures means were calculated separately for the left and right hands. The arithmetic mean of of the fingertip temperature measurements is described hereinafter as "fingertip temperature". Similarly, the arithmetic sums of the temperatures in the wrists of the hands were calculated separately for the left and right hand. The arithmetic mean of the temperature measurements in the wrists of the hands is described later in the manuscript as "temperature in the wrist". The arithmetic mean of the temperature measurements taken over the AVF is described later in the manuscript as "temperature over AVF". Directly after the thermal images of the hands were taken, the subjects had their body temperature measured in the outer ear using a professional medical thermometer. The body temperature measurement thus obtained is described in the remainder of the manuscript as "ear canal temperature". The data obtained were correlated with laboratory blood tests performed at the commencement of dialysis, during routine, periodic examinations. The results of the laboratory tests were performed from the period, when thermal imaging was measurements.were recorded. Table 1 presents the reference values of selected blood laboratory tests routinely performed for haemo- dialysis patients in our center.

Laboratory tests were performed in the hospital laboratory immediately after blood sampling. The calcium-phosphate index was calculated from the calcemia and phosphatemia measurements. In addition, the results of temperature measurements were correlated with data from the medical history of cardiovascular complications and the mortality of patients over the period of time studied (in the period from August 2015 to August 2019). Nicotinism has been defined as either currently smoking, or ever having smoked for a minimum period of 5 years. Past cardiovascular dis-

Table 1.
Reference values of selected blood laboratory tests

Variable	Range of reference values in a healthy population
Serum creatinine [µmol/L]	53–115
Hb [g/dL]	7.5-11.2
PTH [pg/ml]	10-60
Serum calcium [mg/dL]	8.5-10.5
Serum phosphate [mg/dL]	2.9-5.4
FA [IU/L]	30-120
PCT [ng/mL]	<0,5
CRP [mg/L]	<5.0
Serum protein [g/dL]	6.0-8.0
Serum albumin [g/dL]	3.5-5.0
Total cholesterol [mg/dL]	<190
HDL-cholesterol [mg/dL]	=40
LDL-cholesterol [mg/dL]	<115
Triglycerides [mg/dL]	35-160

Abbreviations:
CRP - C-reactive protein; FA - alkaline phosphatase;
Hb - haemoglobin; HDL – high density lipoprotein;
LDL – low density lipoprotein; PCT - procalcitonin;
PTH – parathyroid hormone

Table 1.
Demographic, clinical data and laboratory tests of the investigated subjects

Variable	min-max	Mean ± SD
Age [years]	18-89	64.7 ±15.2
BMI [kg/m^2]	16.06-44.87	25.94 ± 6.81
Total dialysis time * [months]	19-132	66.4 ± 26.8
Serum creatinine [umol/L]	335.9-1255.3	645.3 ± 527.8
Hb [g/dL]	7.1-13.1	10.38 ± 1.35
PTH [pg/ml]	15.5-1385	378 ± 354
Serum calcium [mg/dL]	7.4-10	8.4 ± 0.6
Serum phosphate [mg/dL]	3.2-7.8	5.0 ± 1.2
FA [IU/L]	37-281	110.0 ± 59.7
PCT [ng/mL]	0.04-0.66	0.21 ± 0.15
CRP [mg/L]	0.5-97	13.9 ± 19.4
Serum protein [g/dL]	4.5-7.4	6.5 ± 0.7
Serum albumin [g/dL]	2.2-6.9	3.7 ± 0.8
Total cholesterol [mg/dL]	94-268	155.9 ± 44.2
HDL-cholesterol [mg/dL]	25-61	40.6 ± 7.4
LDL-cholesterol [mg/dL]	28-159	87.4 ± 35.1
Triglycerides [mg/dL]	58-441	146.6 ± 83.9

Abbreviations:
CRP - C-reactive protein; FA - alkaline phosphatase; Hb - hemoglobin; HDL - high density lipoprotein; LDL - low density lipoprotein; PCT - procalcitonin; PTH - parathyroid hormone;
* Total dialysis time - the time from the beginning of dialysis to the end of follow-up or until the patient's death.

ease was defined as a condition following myocardial infarction, angioplasty with or without coronary stent implantation, coronary artery bypass grafting, and coronary artery disease as diagnosed on the basis of cardiological consultation.

Statistical analysis

Data analysis was performed with STATISTICA 13.1 software (StatSoft Inc., Tulsa, OK, USA). Continuous variables are presented either as a mean and standard deviation (SD) or as a median and interquartile range (IQR). Categorical variables are presented as numbers and percentages. The Shapiro-Wilk test was used to determine distribution normality. Categorical variables were compared using the $\chi 2$ test, while continuous variables Student's t-test or the Mann-Whitney U-test (Kruskal-Wallis and multiple repetition tests) as appropriate. The Pearson correlation test (Pearson's r) and the Spearman's rank correlation test (after prior arranging the results) were calculated for the correlation of parametric (continuous) variables. To determine the relationships between continuous variables we used best of regression models (linear, power, logarithmic, exponential). The significance level was set at $p < 0.05$.

Results

The study involved 34 chronically hemodialysed patients over 18 years of age. Table 2 presents clinical, demographic and testing data to describe the study group. Selected clinical, demographic data and laboratory tests performed in study population are presented in Table 2.

Table 3 shows the percentage of hemodialysis patients by gender, type of vascular access (AVF or catheter), co- morbidity and mortality and p-value for the Mann-Witney U test comparing the distribution of respective temperatures in groups. Among the patients diagnosed with diabetes, 2 people suffered from type 1 diabetes, while 16 people had type 2 diabetes. In the examined group of patients, a history of amputation at thigh, lower leg or toe was observed in 2 patients with atherosclerosis of the lower limbs and in 3 patients with diabetic foot.

Using the Mann-Withney U test, we determined whether there were statistically significant differences between the groups when comparing the clinical data with the temperature measurements. Significantly higher ear canal temperature values were observed in patients on dialysis who smoked cigarettes compared with non-smokers (medians: 36.8 vs 36.5 °C, respectively) and in turn, in those dialyzed with catheter compared with those dialyzed using AVF (medians: 36.9 vs 36.5 degrees C, respectively). In people dialyzed using AVF, significantly lower temperatures were observed in the thermal imaging of the fingertips of both hands compared with patients dialyzed with catheter (medians in the right hand: 30.4 vs 33.8 °C and medians in the left hand: 31.8 vs 34.0 °C, respectively). In addition, patients with diabetes had significantly lower temperatures recorded above their AVF than patients without comorbid

Table 3
The p - value for the Mann-Whitney U test between temperature measurements measured in degrees C and certain clinical data.

Site of temperature measureent	Sex: Female	Catheter Dialysis	Dialysis via AVF	Smoking	DM	Cardio-vascular Diseases	history of stroke	Amputation	Death
	n=13 38.2%	n=10 29.4%	n=24 70.6%	n=10 29.4%	n=18 52.9%	n=19 55.9%	n=12 35.3%	n=5 14.7%	n=17 50%
ear canal temperature	0.59	0.02*	0.07	0.04*	0.15	0.14	0.25	0.18	0.12
1	0.83	0.1	0.05*	0.78	0.73	0.54	0.64	0.9	0.52
2	0.82	0.14	0.07*	0.98	0.96	0.83	0.64	0.73	0.42
3	0.74	0.95	0.68	0.921	0.44	0.65	0.85	0.53	0.47
4	0.4	0.8	0.37	0.820	0.25	0.68	0.79	0.33	0.53
5	0.36	0.15	0.44	0.942	0.02	0.1	0.96	0.61	0.68

Abbreviations: AVF - arteriovenous fistula; ; DM – diabetes mellitus;
measurement sites:
1=Fingertip temperature at the side withoutAVF 2=Fingertip temperature at the side with an AVF
3=Wrist temperature at the side without AVF 4=Wrist temperature at the side with AVF
5=Temperature in the area of AVF
*- Statistical significance

Table 4
Results of temperature measurements (° Celsius) in the entire population.

Site of temperature measurement [°C]	Average ± SD	Median (q2-q3)	Min.	Max.
Ear canal temperature	36.6 ± 0.5	36.6 (36.3-36.9)	35.4	37.4
Fingertip temperature at the side without AVF	32.0 ± 2.9	32.6 (30.6-34)	25.5	36.1
Fingertip temperature at the side with an AVF	31.5 ± 3.0	32.7 (28.2-34.3)	26.4	35.4
Wrist temperature at the side without AVF	33.6 ± 1.6	33.7 (33.1-34.6)	29.4	36.2
Wrist temperature at the side with AVF	33.8 ± 1.5	33.9 (32.7-34.6)	29.4	36.9
Temperature in the area of AVF	35.1 ±1.6	35.1 (34.3-36.1)	30.1	38.1

Abbreviations: AVF - arteriovenous fistula;.

Table 5.
Statistically significant differentiation of selected clinical data and laboratory tests in groups of dialyzed patients sub-divided according to the type of vascular access (catheter or AVF).

Variable	catheter			AVF			p-value
	median	q2	q3	median	q2	q3	
Body weight [kg]	62.0	51.0	70.5	75.0	64.0	89.0	0.025
Ca x P [mg/dl]	36.0	30.4	40.0	44.4	34.4	53.9	0.033
CRP [mg/L]	15.3	8.1	30.6	6.4	3.0	12.6	0.012
pH	7.30	7.28	7.34	7.36	7.32	7.39	0.024

Table 6
Statistically significant differences in selected clinical data and laboratory tests between groups of dialyzed patients sub-divided according to the co-occurrence of diabetes

Variable	No diabetes			Diabetes			p-value
	median	q2	q3	median	q2	q3	
Total dialysis time [months]	84.0	53.0	101.5	56.5	46.0	69.5	0.025
PCT [ng/mL]	0.24	0.15	0.41	0.11	0.08	0.17	0.001
Serum albumin [g/dL]	4.0	3.5	4.15	3.55	3.1	3.9	0.043
HDL-cholesterol [mg/dL]	43.0	39.0	45.0	39.0	34.0	41.0	0.020
Temp. AVF [° C]	36.1	35.1	36.6	34.7	34.2	35.6	0.024

Abbreviations: Total dialysis time * - time from the beginning of dialysis to the end of observation or until the patient's death; Temp. AVF – temperature measurements on the upper limb with arteriovenous fistula; PCT - procalcitonin; q2 - second quartile; q3 - third quartile.

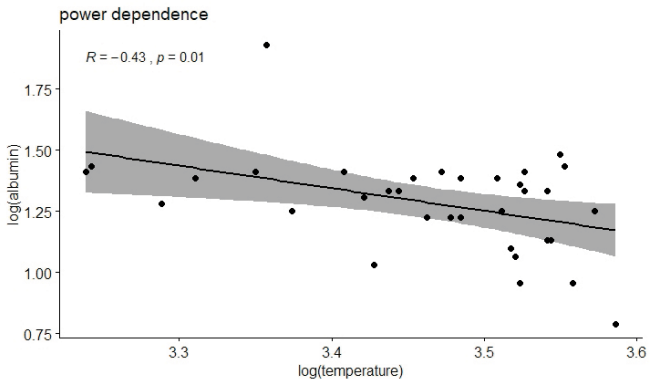

Figure 3
Diagram showing the power dependence of serum albumin concentration on the average right fingertip temperature in the study population.

diabetes (medians: 34.7 vs 36.1 degrees C, respectively). Detailed results of these analyses are presented in Table 2.

In addition, all patients with nicotinism were dialyzed with the catheter (n = 10, 100%). Due to significantly lower average AVF fingertip temperature results in patients dialysed with AVF, we checked the correlation of AVF fingertip temperature with clinical data and laboratory tests. No statistically significant correlation was observed between mean AVF fingertip temperatures and any of the clinical and laboratory variables we tested ($p > 0.05$).

Due to the significantly lower temperature over the AVF in patients with diabetes, we checked the correlation of the temperature over the AVF with clinical data and laboratory results in this group of patients. There were no statistically significant correlations of temperature over AVF with any of the clinical and laboratory variables we examined ($p > 0.05$).

Since the analysis of the correlation between the albumin level and temperature showed a strong linear relationship between the logarithms of the values of these features, therefore by examining different regression models (linear, power, logarithmic, exponential) , it was observed that the power-regression model was the best-fit for describing the effect of serum albumin concentration on the average right-hand fingertip temperature (without arteriovenous fistula) in the entire study population ($n = 34$, $F = 7.4$; $p = 0.01$, $R = - 0.43$). The Shapiro-Wilk for residual showed that the residuals are normally distributed, the Durbin-Watson test showed that there is no autocorrelation of residuals. This model is shown in Figure 3.

Discussion

To our knowledge, the research is the only one in the literature describing the correlation of thermal imaging based hand temperatures with blood tests indicating the risk of cardiovascular complications in patients under chronic hemodialysis. We originally planned to investigate the clinical usefulness of thermal imaging in cardiovascular complications in patients with chronic hemodialysis. The pathophysiological basis of our research hypothesis was the observation that in patients with end stage kidney disease, hypersecretion of PTH may be followed by cardiovascular complications, and is consequently associated with high morbidity and mortality among renal failure patients [16, 17]. In patients with chronic hemodialysis, pathologic calcium-phosphate deposits can be observed in the intima and media of the blood vessels, at sites where the atherosclerotic process, which is frequently observed in the general population, also appears. Medial calcification of blood vessels, known also as Monckeberg's arteriosclerosis or calciphylaxis, is commonly seen in dialysis patients [18, 19]. These processes may lead to a deterioration of blood supply to the tissues, which may result in a decrease in the temperature measured in hemodialysed patients' hands.

The decrease in average fingertip temperature with AVF observed in our study may support our assumption. Haemodialysis is possible due to a vascular access either in form of a central venous catheter or an AVF. In our study, most of subjects had a fistula Cimino-Brescia fistula in the left wrist. After performing AVF in this location, blood is stolen from the superficial palmar arch [20]. Hence, our observation of a lower average temperature of the fingertips in subjects with the wrist AVF suggests diagnosis of subclinical ischemic steal syndrome (ISS) of the fingertips with AVF. In the study of Allen J I et al. and Pietrzyk JA et al. it was observed that thermovision can be an effective method in the assessment of arterial venous fistula function in hemodialyzed patients [9,11].

In addition, the significantly lower average skin temperature over the AVF that we observed in patients with diabetes might also be explained by a greater calcification of the fistula vessels in this group of patients compared with patients without comorbid diabetes. But such a hypothetic explanation needs confirmation by an imaging study that provides qualitative and quantified data on calcium deposits in fistula vessels. The influence of diabetes on calcification of fistula vessels is described by other researchers [21]. In the study of Al Shakarchi J et al., thermal imaging was used to assess the AVF function in the perioperative period [1].

From a clinical perspective, it is interesting to observe a significantly lower average hand temperature in people dialysed with AVF, who also exhibited higher serum albumin levels and body weight, two markers of malnutrition, and lower concentration of the inflammation marker CRP than observed in patients dialysed with the catheter. The trias malnutrition-inflammation-atherosclerosis (MIA) is considered as non- traditional risk factors for cardiovascular complications and death in renal failure patients under chronic hemodialysis [22]. In our study, patients undergoing hemodialysis with the catheter had significantly lower body weight, higher CRP, lower serum albumin and a higher temperature in the fingertips of both hands.

Additionally in our study, we observed that with a decrease in the concentration of serum albumin, the average temperature of the fingertips of the hand without a fistula also significantly decrease. The concentration of albumin in blood serum is one of the components tested in suspicion of MIA syndrome [22]. The regularity of the correlation observed in our study may be usefulness in clinical practice in differettial diagnosis of the risk of MIA syndrome in chronic hemodialysis patients.

The results of our research, in particular the correlation of hand temperature with the components of MIA syndrome, should be confirmed in a larger group of patients with hemodialysis, taking into account the selected thermal imaging temperature measurement sites presented in our work. In future studies, it would be advisable to verify the lower temperature over the AVF in diabetic patients, by measuring the blood flow through the AVF by using such as power Doppler ultrasound. .

Limitations of the study

The limitations of the study are relatively small number of patients included in the study, limited technical capabilities of thermal imaging cameras, lack of application of the adopted consensus of thermographic studies in the study methodology, which results from the experiment carried out two years before these recommendations were published in 2017 [23].

Conclusions

Given the higher average temperature of the fingertips measured in patients with chronic hemodialysis, non-invasive, reproducible, and relatively inexpensive thermal imaging may be a screening method for patients at risk of malnutrition-inflammation-atreosclerosis syndrome.In haemodialyzed patients with AVF, a lowered temperature of the fingertips of the fistula hand may be an expression of subclinical ischemia of this hand. Thermal imaging of the hand is not useful in the assessment of cardiovascular complications or of the risk of death in patients on chronic dialysis during a four-year follow-up period.

Acknowledgement

We like to thank the editor Dr Kurt Ammer and the three reviewers of this article for their constructive criticism and valuable proposals to improve our manuscript.

References

1.Shakarchi JA, Hodson J, Field M, Inston N. Novel use of infrared thermal imaging to predict arteriovenous fistula patency and maturation. J Vasc Access 2017; 18(4): 313-318.

2.Woodhead GS, Varrier-Jones PS. Clinical Thermometry, Lancet, 1916.

3.Lawson R. Implications of surface temperatures in the diagnosis of breast cancer. Canadian Medical Association Journal, 1956; 75: 309-10.

4.Ammer K. The sensitivity of infrared imaging for diagnosing Raynaud's phenomenon and for Thoracic Outlet Syndrome is dependent on the method of temperature extraction from thermal images, Thermology International, 2008; 18: 81-88.

5.Spalding SJ, Kwoh CK, Boudreau R. et al. Three-dimensional and thermal surface imaging produces reliable measures of joint shape and temperature: a potential tool for quantifying arthritis, Arthritis Res Ther, 2008; 10: R10.

6.Lahiri BB, Bagavatiapphan S, Jayakumar T, Philip J. Medical applications of infrared thermography: A review, Infrared Physics & Technology, 2012; 55: 221-35.

7.Ring EFJ, Ammer K. Infrared Thermal Imaging in Medicine. Physiol Meas 2012; 33: R32-R46

8.Maca T, Schmaldienst S, Atteneder M et al. Infrared thermography for control of hemodialysis shunts, Proc. 19th Annu. Int. Conf. of the IEEE Engineering in Medicine and Biology Society 1997; 2: 621-624.

9.Allen J, Oates CP, Chishti AD, Ahmed IAM, Talbot D, Murray A. Thermography and colour duplex ultrasound assessments of arterio-venous fistula function in renal patients. Physiol Meas 2006; 27: 51-60.

10.Czupryniak A, Kaluzynska A, Nowicki M et al. Phenomenon and endothelial dysfunction in end-stage renal disease patients treated with hemodialysis, Kidney Blood Press Res 2005; 28: 27-31.

11.Pietrzyk JA, Korohoda P, Krawentek L, Drozdz D, Zachwieja K, Miklaszewska M. Thermography as an introductory method for evaluation of vascular access in hemodialysed subjects, Pediatric Review, 2004; 34: 119-124.

12.Booth K, Steven H. Optoelectronics. Wydawnictwo Komunikacji i Lacznosci, Warszawa 2001; [in Polish].

13.Infrared Themography R300, User manual, NEC Avio Infrared Technologies Co. Ltd., 2011.

14.Maraj M, Kusnierz-Cabala B, Dumnicka P, et al. Redox Balance Correlates with Nutritional Status among Patients with End-Stage Renal Disease Treated with Maintenance Hemo- dialysis. Oxid Med Cell Longev. 2019; 2019: 6309465.

15.Choi SR, Lee YK, Cho AJ, et al. Malnutrition, inflammation, progression of vascular calcification and survival: Inter-relationships in hemodialysis patients. PLoS One. 2019; 14(5): e0216415.

16.Wood C, González EA, Martin K.J. Challenges in the therapy. of secondary hyperparathyroidism. Ther Apher Dial 2005; 9: 4-8

17.Speer MY, Giachelli CM. Regulation of cardiovascular calcification,.Cardiovascular Pathology 2004; 13: 63-70.

18.Moe SM, Chen NX. Mechanisms of vascular calcification in chronic kidney disease, J Am Soc Nephrol, 2008; 19: 213-216.

19.Stompór T. An overview of the pathophysiology of vascular calcification in chronic kidney disease, Perit Dial Int 2007; 27: 215-222.

20.Brescia MJ, Cimino JE., Appel K, Hurwich BJ. Chronic hemodialysis using venipuncture and a surgically created arteriovenous fistula. N Engl J Med 1966; 275(20): 1089-1092.

21.Jankovic A, Damjanovic T, Djuric Z, et al. Impact of vascular calcifications on arteriovenous fistula survival in hemodialysis patients: a five-year follow-up. Nephron, 2015; 129(4):247-252.

22.Stenvinkel P, Heimburger O, Lindholm B, Kaysen GA, Bergstrom J. Are there two types of malnutrition in chronic renal failure? Evidence for relationships between malnutrition, inflammation and atherosclerosis (MIA syndrome).Nephrol Dial Transplant 2000;15: 953-960.

23.Moreira DG, Costello JT, Brito CJ, et al. Thermographic imaging in sports and exercise medicine: A Delphi study and consensus statement on the measurement of human skin temperature. J Therm Biol. 2017;69:155-162.

Address for Correspondence

Wociech Zylka

The Didactic Centre of Technical and Natural Sciences,
College of Natural Sciences, University of Rzeszów
1 Prof. St. Pigon Street
35-310 Rzeszów, Poland
e-mail: wzylka@urz.edu.pl, wojzyl@op.pl

(Received: 06.07.2020, revision accepted 28.10.2020)

Employment of FLIR ONE Infrared Cameras in Medicine - A literature overview

Kurt Ammer

European Association of Thermology, Vienna, Austria
Faculty of Applied Mathematics and Computing, University of South Wales, Treforest Campus, Pontypridd, UK

SUMMARY

There is considerable interest in using low cost, smartphone based infrared cameras for medical imaging such as the FLIR ONE A screening search in Google Search retrieved more than 1200 hits for the search term "FLIR ONE"A search in all data fields of the database Scopus resulted in 137articles. Limiting the search to "medicine" resulted in 71 articles. A special focus of this overview article is whether the conditions and methods for evaluation of thermal images were completely reported. The FLIR ONE was applied in both human and veterinary medicine. Studies have been conducted in a wide range of medical disciplines, predominately in surgery, but also in diabetic foot research, rheumatology, physical/sports medicine, anaesthesiology, allergology, senology and animal experiments. 9 articles had their focus on the performance of the FLIR ONE reporting either the accuracy or the reliability of temperature measurements performed with the smartphone based infrared camera. The performance of the device was poor to fair in obtaining absolute temperature values, but moderate to good when temperature differences were assessed. The qualitative evaluation based on the distribution and colours of the false-coloured thermal image was described as excellent. Smartphone based infrared cameras may have a place for quick documentation of unexpected thermal phenomena.

KEY WORDS: medical thermography, FLIR ONE, low-cost infrared camera, smartphone based

DER EINSATZ VON FLIR ONE INFRAROT-KAMERAS IN DER MEDIZIN - EIN ÜBERBLICK

Zur Zeit findet sich ein beträchtliches Interesse am Einsatz von kostengünstigen, Mobiltelefon gestützten Infrarotkameras zur medizinischen Bildgebung wie z.B. die FLIR ONE. Eine orientierende Literatursuche in Google Scholar fand für den Begriff "FLIR ONE" mehr als 1200 Einträge. Die Beschränkung der Suche auf "Medizin" führte zu 71 Artikeln. Ein besonderer Schwerpunkt dieses Übersichtsartikels ist, ob die Bedingungen und Methoden zur Bewertung von Wärmebilder vollständig berichtet wurden. Der FLIR ONE wurde sowohl in der Humanmedizin als auch in der Veterinärmedizin angewendet. Die Studien wurden in einer breiten Palette medizinischer Disziplinen durchgeführt, vorwiegend in der Chirurgie, aber auch in der Forschung über den diabetischen Fuß, Rheumatologie, Physikalische/ Sportmedizin, Anästhesiologie, Allergologie, Senologie und Tierversuche. 9 Artikel hatten ihren Schwerpunkt auf der Leistung der FLIR ONE, die entweder die Genauigkeit oder die Zuverlässigkeit von Temperaturmessungen mit der Smartphone-gestützten Infrarotkamera berichteten. Die Leistung des Geräts war bei der Erlangung absoluter Temperaturwerte schlecht oder gering, aber mäßig bis gut, wenn Temperaturunterschiede bewertet wurden. Die qualitative Bewertung auf Basis der Verteilung und der Farben des falsch-farbigen Wärmebildes wurde als ausgezeichnet beschrieben. Smartphone-basierte Infrarotkameras können einen Platz für eine schnelle Dokumentation unerwarteter thermischer Phänomene haben.

SCHLÜSSELWÖRTER: medizinische Thermografie, FLIR ONE, kostengünstige Infrarotkamera, Mobiltelefon gestützt

Thermology international 2020, 30(4) 128-145

Introduction

There is considerable interest in using low cost, smartphone based infrared cameras for medical imaging. A screening search in Google Scholar revealed for the search term "FLIR ONE" more than 1200 hits. A closer look on this result found that about 45 % of the articles were related to applications in medicine, to both basic medical science and clinical science.

Although the growing popularity of infrared thermal imaging is welcomed and appreciated, some of the published articles are of questionable scientific quality and definitely do not meet criteria of "Good Clinical Thermographic Practice", a framework formed by standard procedures for infrared image capture and evaluation in combination with employed infrared cameras that meet the minimum requirements for accurate and reliable temperature measurement. Consequently, the suitability of FLIR ONE cameras for medical applications was questioned [1]. Alfieri et al. reported poor agreement of absolute regional skin temperatures obtained with a FLIR T650SCR or a FLIR ONE iOS [2]. A recent study investigating the performance of smartphone attached infrared cameras, excluded FLIR ONE Pro from evaluation due to their small sensor array [3]. In 2004, first generation of FLIR ONE became available, but temperature measurements were qualified as inaccurate despite recently performed calibration [4].

Currently, three models of FLIR ONE IR-Camera are commercially available. Labelled as FLIR ONE- Gen 3, FLIR ONE Pro LT and FLIR ONE Pro, they slightly differ

Table 1
Specifications of the FLIR ONE versions

	FLIR ONE Gen 3	FLIR ONE Pro LT	FLIR ONE Pro
Price	~199-99 $	~299.99 $	~399.99 $
Accuracy	±3 °C or ±5%, typical Percent of the difference between ambient and scene temperature. Applicable 60 sec after start-up when the unit is within 15 °C-35 °C and the scene is within 5 °C -120 °C.		
Non-Operating Temperature	-20 °C – 60 °C (-4°F – 140°F)		
Scene Dynamic Range	-20 °C – 120 °C (4°F -248°F)	-20 °C–400°C (-4°F-752°F)	
Spot Meter	Off / °C / °F. Resolution 0.1°C / 0.1°F		
Weight	34.5g	36.5 g	
Dimensions (H x W x D)	34 x 67 x 14mm (1.3 x 2.6 x 0.6 in)	68 x 34 x 14mm (2.6 x 1.3 0.6 in)	
Phone	iOS, Android (USB-C)	iOS, Android (USB-C) Android (Micro-USB)	
APP			
Adjustable MSX distance	0.3m- Infinity		
Battery charge monitor	0-100%		
Battery charge time	40 min		
Battery life	approximately 1 hour	1 hour	
Capture modes	Video, Still image, lime lapse		
File format: Still image	radiometric jpeg		
File format:Video	MPEG-4 [MOV (iOS), MP4 (Android]	MPEG-4 (MOV)	MPEG-4 (MP4)
Palette	Gray (white hot), Hottest, Coldest, Iron, Rainbow, Arctic, Lava and Wheel.		
	Contrast	Rainbow HC	
Image Presentation Modes	MSX (only)	Infrared, visual, MSX. gallery	
VixidIR Image Enhancement	No	Yes	
Video and Still ImageDiaplav Capture	Saved as 1440x1080		
ENVIRONMENTAL & APPROVALS			
Emissivity Settings	Matte: 95%, Semi-Matte: 80%, Semi-Glossy: 60%, Glossy: 30%		
	Reflected background temperature is 22°C		
Mechanical shock	Drop from 1.5m	Drop from 1.8m	
Operating Temperature	0 °C-35°C (32°F-95°F) - battery charging 0 °C-30 °C(32°F-86°F)		
IMAGING & OPTICAL			
Focus Fixed	15cm-Infinity		
Frame Rate	8.7Hz		
HFOV/VFOV	50°± 1°/38° ± 1°	55°± 1°/43° ± 1°	
Shutter	Automatic/Manual		
Thermal Resolution	80 x 60	120 x 80	
Thermal Sensor : Pixel size	17 μm	12 μm	
Thermal Sensor Spectral range	8- 14μm		
Visual Resolution	1440 x 1080		
Thermal Sensitivity (NEDT)	150mK	100mK	70mK

https://www.flir.com/products/flir-one-pro/ last accessed 11.11.2020
https://www.flir.com/products/flir-one-pro-lt/ last accessed 11.11.2020
https://www.flir.com/products/flir-one-gen-3/ last accessed 11.11.2020

in basic specifications and extra features. In all types, a visual camera image supports the visual quality of the displayed thermal image by using different technologies for image enhancement. While the most advanced model FLIR ONE PRO is equipped with a sensor of 120 x 80, 12μm sized pixels and a NEDT of 70mK, the basic FLIR ONE Gen 3 and the intermediate model FLIR ONE Pro LT use the 80 x 60 sensor with a pixel size of 17 μm, with a thermal sensitivity of 150mK for the basic and 100mK for the intermediate model. 4 fixed levels of emissivity (0.95, 0.8, 0,6 and 0.3) can be set for thermal imaging. For immediate temperature measurements spot meters with a sensitivity of 0.1°C are available in all models. Radiometric JPGs can be exported for offline evaluation with dedicated software. Table 1 shows the specifications of the current FLIR-ONE models.

Validity and reliabilty

Since the terms validity and reliability appear often in medical imaging articles, the definition of these constructs used

in research and science to confer quality assurance. Validity is often synonymously used for accuracy which is slightly different defined in metrology, computer science or clinical science. In metrology, **accuracy** is defined as *"closeness of agreement between a measured quantity value and a true quantity value of a measurand*". A measurement is said to be more accurate when it offers a smaller measurement error.
Measurement error is defined as "*measured quantity value minus a reference quantity value*". For example, someone is measuring with an infrared radiometer the blackbody source temperature of 30°C as 30.4°C, thus the measurement error of the radiometer is +0.4°C. The measurement error should not be confused with the term "**uncertainty**" "*non-negative parameter characterizing the dispersion of the quantity values being attributed to a measurand*". From a series of measurements, the average value of all measurements can be calculated, and the corresponding **standard deviation** represents the dispersion of the measurement. In the case, that a stable reference quantity of neglectable uncertainty is measured, the standard deviation is identical to the **standard error of the mean** (SEM), but this does not apply to the quantification of unstable references of small to large dispersion measures.

In medicine, **diagnostic accuracy i**s based on the detection rate of properties with an experimental method in comparison to the standard method. This results in 4 classes of findings, **true positives** (**TP),** when the method indicates the presence of a feature, that is truly present; **true negatives (TN)**, when the method describes the absence of a property, that is truly absent; **false positives (F**P), when the method indicates the presence of a feature, that is truly absent and **false negatives (FN**), when the method describes the absence of a property, that is truly present. These four classes are used to calculate **sensitivity** also named **recall** or hit rate, which is equal to the rate of true positive cases, TP/(TP+FN). **Specificity** is equal to the rate of true negative cases, TN/(TN + FP), and represents the proportion of tested subjects who are free of the marker of interest, which means in medicine, that they are not diseased. **Diagnostic accuracy** is expressed as a proportion of correctly classified subjects (TP+TN) among all subjects (TP+TN+FP+FN). Like **predictive values**, the diagnostic accuracy depends on the prevalence of the condition of interest. **Prevalence** is equal to the number of positive cases in the population. With the same sensitivity and specificity, the diagnostic accuracy of a particular test increases as the disease prevalence decreases. The performance of a binary classification test can be measured with the **positive predictive value** also known as **precision**. It is calculated as TP/(TP + FP); that is equal to the proportion of true positives among all positive results.

In computer science, particularly in pattern recognition, information retrieval or classification (machine learning), sensitivity and specificity are determined in a similar way as in medicine. This may result in confusion between the accuracy of a computer programme to correctly detect a feature used for diagnosis and the performance of such a computer programme for correct identification of this feature in a population of patients. Another source of confusion arises from labelling the positive predictive value as precision when testing the performance of classification procedures.

Occasionally the terms accuracy and precision are erroneously used interchangeable. In everyday language reliability is a condition that can be trusted because it is valid and regular. In metrology, reliability is termed "**precision"** defined "*as closeness of agreement between indications or measured quantity values obtained by replicate measurements on the same or similar objects under specified conditions*". Different conditions of repeated measurements define r**epeatability precision**, intermediate measurement precision, and **reproducibility precision**. Be aware, that accuracy is also based on repeated measurements, thus, the conditions of measurement is equally important for the determination of both accuracy and precision.

Repeatability condition is a "*condition of measurement, out of a set of conditions that includes the same measurement procedure, same operators, same measuring system, same operating conditions and same location, and replicate measurements on the same or similar objects over a short period of time*".

Reproducibility condition is defined "*as a condition of measurement, out of a set of conditions that includes different locations, operators, measuring systems, and replicate measurements on the same or similar objects*".

Following these definitions, comparing the temperatures obtained with two cameras is a reproducibility study irrespective whether they are of the same model of the same manufacturer or different models from the same or different manufacturer. Repeated evaluation of a set of thermal images by the same reader, with same equipment within the same environment is labelled as repeatability study when repeated within 24 hours. A longer time interval and involving other operators or measuring systems or the use of equipment altered by calibration defines the determination of intermediate measurement precision. According the provided definition, repeatability of thermal imaging in humans or animals is difficult to define, due movement artifacts.

Vardasca reported already some applications of FLIR ONE in medicine [1]. The aim of this article is to provide an updated overview on articles reporting the use of FLIR ONE in the medical field. A secondary aim was to analyse medical articles, whether the reported conditions of image recording allow to classify the imaging as a measuring procedure.

Method

A screening search in Google Scholar revealed for the search term "FLIR ONE" more than 1200 hits. A closer look on this result found that about 45 % of the articles

were related to applications in medicine. As next step a search in the data base Scopus was performed with the search term "FLIR ONE" in all fields without limitation to type, language and year of publication revealing 137 hits. Refinement to "medicine" resulted in 71 articles, allocated to the subject areas "Medicine" (39 hits) "Computer Science" (18 hits). "Engineering" (12 hits) "Biochemistry, Genetics or Molecular Biology" (10 hits), "Physics and Astronomy" (7 hits), "Materials Science" (6 hits), "Health Professions" (5 hits), "Mathematics" (4 hits), "Agricultural and Biological Sciences" (3 hits). Chemistry, Energy, Multidisciplinary and Nursing revealed 2 hits each and 1 hit each was obtained for Decision Sciences, Immunology and Microbiology, Neuroscience, Veterinary.

The abstracts of all 71 articles were read and data were extracted on type of article, study aim, application of thermal imaging for diagnosis or as an outcome measure, medical diagnosis, sample size of investigated subjects. Since abstracts often do not provide all details on study methods, full versions of the articles were retrieved whenever possible. To understand the conditions of thermal imaging, attention was focused on the methods section of included articles and 6questions were checked:

1. Did the authors report the ambient temperature during image capture?

2. Was the smartphone held in hands or mounted on a kind of tripod?

3. Was the distance between the camera and the body region of interest reported?

4. Was the evaluation of thermal images qualitatively or quantitatively?

5. Was the inbuilt spot meter or an offline analysis with a dedicated software used for analysis?

6. Were the thermal images compared to any other evaluation method?

The study aims and findings of selected full-length articles reporting experimental studies are presented in tables. In case that the information about the article was restricted to the abstract and other data such as key words, authors affiliation, grants and so on, the key message of the article is presented in the results and their plausibility is discussed.

Results

65 articles published in journals, 5 conference papers and 2 book chapter were considered for evaluation. However, all 137 articles are listed in the section references to provide an overview on other application fields of the FLIR ONE infrared cameras outside of medicine.

Measurement performance of FLIR ONE

Table 2 shows the results of selected articles investigating the measurement performance of the FLIR ONE, and the corresponding table 3 shows the measurement conditions reported.

Curan et al. [4] compared the performance of the infrared radiometer Omega OSXL450, a FLIR E60 and a FLIR ONE in measuring human forehead's temperature before and after two methods of calibration. Both calibration procedures improved the agreement between measurements made with the FLIR E60 and the Omega OSXL450 but did not appear to positively impact measurements made with the FLIR ONE. Two other studies investigating the accuracy of FLIR ONE measurements against a stable reference, one conducted in Portugal [1] and the other by British-Polish cooperation [65].

Four FLIR ONE Gen 2, two of them iOS based and two attached to Android systems, were exposed to a start-up drift test with a reference temperature of 30°C and a temperature sweep from 20 to 40° that was executed 5 times [1]. In the start-up drift test the mean temperature obtained by the 4 cameras wa s by 0.9 ± 0.2 °C higher than the black body temperature. Over the temperature range from 20 to 40°C, the mean bias of all measurements was 0.91°C with limits of agreement of -0.2 to 2.03°C. Despite the excellent reliability between both FLIR ONE versions and the blackbody source, and between the devices with ICCs ≥0.991, due to the wide span of limits of agreement the device is not recommended for medical application when absolute temperature values are mandatory.

The accuracy of 5 infrared cameras (including FLIR ONE) employed in equine thermography was tested against a blackbody source [70]. The FLIR ONE device exhibited considerable variability in output during the warmup, and by the end of the warmup period it was under-reading the blackbody temperature by 1.2 °C. Like the other 4 tested imagers, the FLIR ONE exhibited an offset from the true blackbody temperature which varied with blackbody temperature. The FLIR ONE slightly overestimated the temperatures 20°C to 23°C, 25°C and 26°C, but under-read all other temperatures with higher deviations at 36°C to 40°C. The authors concluded that variations in performance were responsible for the cameras contributing almost 83% of the variance in the thermographic temperature measurements, but the contribution of specific imagers was not investigated.

A study investigating the reliability of wound size measurement of a smartphone app in comparison to planometry included also wound temperature measurements with either a FLIR ONE camera or the infrared thermometer Exergen DermaTemp 1001 [5]. However, the obtained non- significant paired t-test must not be interpreted in a way, that the temperature readouts of both devices are interchangeable.

Bilateral index finger temperature measurements were obtained in 30 healthy participants using the infrared thermometer Exergen DermaTemp 01001RS and FLIR ONE attached to an iPhone 7 Plus [6]. Measurement conditions such as room temperature, measurement site on the index,

calibration of the devices were not reported. Intraclass correlation coefficient of repeatability was higher for the infrared camera than for the radiometer measurements in side-to-side differences. The bias of agreement of side-to-side differences recorded with either device was 0.56°C (limits of agreement(LOA) -1.09°C to 2.20°C) and for individual side measurements: 2.64°C (LOA, 0.96°Cto 4.32°C), respectively. However, there are severe concerns about the accuracy of temperature measurements performed, since the authors provided as an example for the facilities of infrared imaging a thermogram of a hand after failed replantation of the small finger. In this FLIR ONE thermal image, a temperature as much as 37.7°C(!) is displayed at the unaffected fingertip of the index.

A frequently quoted a Japanese study evaluated thermal images recorded with the FLIR ONE or the hand-held Thermotracer TH 8700N reported absolute intra-device, intra-rater and inter-rater reliability of temperature readouts based on kappa statistics [7]. An extended conference abstract compared various infrared sensors to a contact thermal sensor, but unclear descriptions of measurement methods, measured quantities and their units does not allow to follow the argumentation, that FLIR ONE achieved the best results in this comparison [8].

Alfieri et al. investigated whether regional skin temperatures obtained in 10 locations of the lower extremity with a FLIR T650SCR infrared camera can be reproduced by using a FLIR ONE Pro iOS [2]. Since the mean difference of corresponding ROIs was less than 0.5°C, for all imaged anatomical of the lower extremities thermal symmetry was confirmed with both cameras. There was poor agreement of absolute temperatures obtained by the FLIR T650SCR compared to FLIR ONE with a bias of -1.2 ± 2.9 (LOA -6.9 to 4.4 °C).

In a cross-sectional observation study with 32 patients suffering from (diabetic) neuropathy, van Doremalen et al. investigated the reproducibility of the temperature difference between plantar feet obtained by a FLIR ONE Gen 2 or a FLIR SC305 [9]. The authors concluded from ICC-values of 0.987 for the total foot and of 0.981 for the combined pre-specified regions and the small mean bias of the temperature difference between the two measurements on excellent agreement and interchangeability of temperature measurements obtained with either device. Although the span of agreement was 1.75°C for the total foot and 2.7° for combined regions within the cameras' specifications for accuracy of ± 2.0°C, this range of possible variations in temperature does not allow to recommend to interchange these devices in paired measurements of individual subjects(objects).

Jaspers et al. studied the interrater reliability of temperature difference between the centre of skin burns and a reference area of unaffected skin recorded with a FLIR ONE Gen 2 at different time points [10]. SEM values between 0.17 and 0.22, and ICC values of 0.999 indicated excellent interrater reliability.

Oliver and coworkers studied the intra-rater and inter-rater reliability of the skin temperature at the midportion of the Achilles tendon recorded with a FLIR E8 and a FLIR One Gen 2 camera positioned at a distance of 0.5 or 1m to the rear foot [11]. There was excellent intra-rater reliability for both cameras at all distances and also excellent inter-rater reliability for FLIR ONE at 0.5 m and for FLIR 8 at 0.5 and 1m. Inter-rater reliability for FLIR ONE at 1m distance was good, but agreement between devices was poor. In a second, recently published study, Oliver et colleagues evaluated the influence of distance and angle of view on the reproducibility of the FLIR ONE recorded skin temperature at the midportion of the Achilles tendon [12]. No significant differences of skin temperatures were found between distances and angles. Effect sizes were trivial to small. Although the bias in temperature was small in all positions compared, their wide limits of agreement warrant caution when comparing temperatures recorded with different camera positions.

Clinical studies

The results of selected clinical studies are shown in table 4 and the measurement conditions reported by these studies are presented in table 5.

Wound healing

Thermal imaging with FLIR ONE cameras in wound management was the topic of 14 articles, but only 9 papers reported clinical studies. Excluded for further consideration were 7 papers including a book chapter providing an overview on porcine models of wound healing[13]. 3 articles reported simulation models s of foot ulcers using external heating of small skin areas in healthy subjects to simulate the thermal precursor of developing ulcers [14, 15, 16). A conference paper was completely dedicated to segmentation of the foot area and did not report clinical data [A conference paper applied FLIR ONE for feeding thermal image data from wounds into a multi-sensor system developed for the care management of pressure ulcers [17]. An article from Romania was excluded since most of the images in a small group of patients with ulcers were not captured with a FLIR ONE camera [18]. A review article on the utility of smartphone applications and technology in wound healing [19], contains a small section on FLIR ONE quoting the articles by Jaspers et al. [10] and Xue et al.[20].

The abstract of a paper from Iran was confusing, since thermal conductivity was mentioned as the outcome of an infrared thermal imaging study [21]. A study from the United States, only available as abstract, compared in 5 patients with acute third-degree burn wounds indocyanine green (ICG) angiography with thermal images. The area of unsalvageable tissue as determined by FLIR ONE closely corresponded to the area determined by ICG. FLIR ONE overestimated unsalvageable tissue margins by approximately 1 to 2 cm [20].

Three articles tried to predict healing time of burn wounds based on thermal images captured with a FLIR ONE camera. While 2 studies related retrospectively thermal images

Table 2
Reliability studies

Author (Publication year)	Research aim	Study type/participants	Comparison	Temperature measurement	Result
Alfieri et al. (2020)	Reproducibility of regional skin temperatures in 10 locations of the lower extremity	Cross-sectional study with 20 healthy subjects	FLIR ONE Pro iOS T650SCR	Rectangular regions of interest defined with FLIR Tools. Mean temperature of ROIs Difference of mean temperatures of corresponding ROIs Thermal symmetry was defined by a temperature difference less than 0.5 °C to the contralateral side.	Poor agreement of absolute temperatures obtained by either device. Thermal symmetry was detected by either device since the mean temperature differences were for T650SCR in the range of 0.005 to 0.12°C, and 0.015 to 0.07 °C for FLIR ONE Pro iOS
Oliver et al. (2020)	Reproducibility of the skin temperature at the midportion of the Achilles tendon	Cross-sectional study with 7 healthy subjects	FLIR One 2 Gen Images were taken at 6 locations resulting in different distances and angles	6cm line traveling though the centre of the midportion of the Achilles tendon using FLIR Research IR MAX	No significant differences of skin temperatures were found between distances and angles. Effect sizes were trivial to small.
Oliver et al. (2019)	Intra-rater and inter-rater reliability of the skin temperature at the midportion of the Achilles tendon	Cross-sectional study with 7 healthy subjects	FLIR One 2Gen FLIR E8	6cm line traveling though the centre of the midportion of the Achilles tendon using FLIR Research IR MAX	Excellent intra-rater reliability for both cameras at all distances. Excellent inter-rater reliability for FLIR ONE at 0.5 m and for FLIR 8 at 0.5 and 1m. Good inter-rater reliability for FLIR ONE at 1m distance. Poor agreement between devices
Vardasca et al. (2019)	Accuracy of temperature measurements against a blackbody Inter-device reliability	Cross-sectional study with 4 cameras	2 FLIR One Gen 2 iOS 2 FLIR One Gen 2 Android	Circular region of interest enclosing the temperature field of the black body source	In the start-up drift test the mean temperature obtained by the 4 cameras was by 0.9 ± 0.2 °C higher than the black body temperature. Over the temperature range from 20 to 40°C, the mean bias of all measurements was 0.91°C with limits of agreement of -0.2 to 2.03 °C ICCs between black body temperature, android and iOS-based cameras indicated excellent reliability
Jaspers et al. (2017)	Interrater reliability of temperature difference determined in thermal images of skin burns	Cross-sectional study with 50 wounds in 41 patients	FLIR ONE Gen 2	FLIR Tools; Mean temperature in circular ROI at the centre of the wound, mean temperature of circular reference ROI located in unaffected skin, at least 3cm apart from the wound edge or on the contralateral limb. Difference between both ROIs. Thermal imaging was performed at T1:day 1 to day 3 after burn T2: day 4 to day 7, T3: day 8 to day 10.	At the time points T1, T2 and T3 SEM values were 0.22, 021 and 0.17, respectively. ICC values of 0.999 indicated excellent interrater reliability. At T1, the mean bias to agreement was -0.1°C with limits of agreement (LOA) from -0.71 to 0.51°C.
Kanazawa et al.(2016)	Inter- and intra-rater reliability of qualitative evaluation of thermal images recorded from ulcers or diabetic feet	Cross-sectional study in 3 patients with sacral pressure ulcers and 5 patients with diabetic foot syndrome	FLIR ONE Thermotracer TH700N(?) (perhaps TH7800N)	Qualitative evaluation	Absolute agreement between both devices and absolute intra- and interrater reliability
van Doremalen et al.-(2019)	Inter-device reliability of the temperature difference between plantar feet	Cross-sectional study with 32 patients	FLIR ONE Gen 2 FLIR SC305 (combined to a Canon EOS 40D for colour photographs)	total area of the plantar foot, nine pre-specified circular ROIs	ICC for the total foot: 0.987, Bland Altman plot: bias -0.14 LOA: -1.0 to 0.75

Table 3
Reported method for thermal imaging in reliability studies

	Ambient temperature	Camera Model (mounting)	Distance to target /image content	evaluation	Tool for temperature measurement	Measure of reliability
Alfieri et al. (2020)	20.9 ± 0.4 °C	FLIR ONE Pro (hand-held) FLIR T650SC (tripod)	4m (lower extremities) Simultaneous image capture	Mean regional skin temperature	FLIR Tools	Concordance correlation coefficient (CCC9 Bland Altman limits of agreement (LOA)
Oliver et al. (2020)	22.2 ± 0.2 °C	FLIR One Gen 2 (tripod)	0.5m with angle of 0°or 14° 1m with angle of 0° or 7°	Mean temperature of a line above the Achilles tendon	FLIR Research IR MAX	Bland Altman limits of agreement (LOA) Cohen´s effect size d
Oliver et al. (2019)	22.2 ± 0.2 °C	FLIR E8 (tripod) FLIR One Gen 2 (tripod)	0.5 or 1m 2 raters of differing experience	Mean temperature of a line above the Achilles tendon	FLIR Research IR MAX	Standard error of measurement (SEM), minimal detectable change (MCD) interclass correlation coefficient (ICC) Bland Altman limits of agreement (LOA)
Vardasca et al. (2019)	4.0 ± 0.3°C	FLIR One Gen 2 Androd (attached to LG400 Pad) FLIR One Gen 2 iOS (attached to mini iPad)	0.3m	Mean temperature of reference source	FLIRThermaCAM researcher 2.10 Pro	Interclass correlation coefficient (ICC) Bland Altman limits of agreement (LOA)
Jaspers et al. (2017)	Outpatient clinic 23.3°C(21.2–26.9) Burn center 23.4°C (19.8–24.8)	LIR ONE Gen 2 attached to an iPad mini, held in hands	0.5 to 1m 2 raters	Temperature difference between both ROIs.	FLIR Tools	Interclass correlation coefficient (ICC) Standard error of measurement (SEM), Bland Altman limits of agreement (LOA)
Kanazawa et al. (2016)	Not reported	FLIR ONE attached to a smartphone Thermotracer TH7800N, both devices held in hands	No distance reported 2 raters	The raters classified the thermal images as a lower or higher temperature at the wound bed than the adjacent skin for the PUs assessment, and as higher temperature at inflammatory area in the diabetic foot.		Cohen's kappa coefficient
van Doremalen et al.-(2019)	Not reported, (images captured in the outpatient clinic)	FLIR ONE Gen 2 attached to Motorola XT1642 Moto G4 Plus smartphone, held in hands FLIR SC305 combined to a Canon EOS 40D, a light module, thermal reference elements and a foot support were mounted in a wooden box	Approximately 1 ± 0.25 m, both feet within the cameras' maximum field of view	Contralateral difference in mean temperature between the total soles and between each of the pre-specified circular ROIs	FLIR ONE app (by Georg Friederich), custom made Matlab software for FLIR SC305	Interclass correlation coefficient (ICC) Bland Altman limits of agreement (LOA)

to the day of observed wound closure [10, 21], the third study related thermal images with laser Doppler images, for which prediction patterns are established [22]. In the early phase of healing, skin burns present with lower temperature than the surrounding non-injured tissue. A wound area colder by approximately 1.2°C predicted healing within 15 days [23]. FLIR ONE was recommended in a letter for the evaluation of burns, but quantitative data for support of this recommendation were not provided [24].

Diabetic foot

A low-quality paper presented non quantified FLIR ONE thermograms from a small group of patients with a high-risk diabetic foot [25]. An article from Peru presented some thermal images merged with photographs from the feet of diabetics but did not report diagnostic results of this evaluation approach [26]. Bouallal et al. proposed techniques for segmenting the plantar foot in thermal images [27]. They also reported the foot temperature behaviour before and after immersion in cold water in three goups with different risk to develop foot ulcers. van Doremalen and coworkers [9] conducted a study in 32 patients with peripheral neuropathy and foot ulcers, which were present in 28 patients, but recently healed in 4 participants comparing foot temperatures recorded with a FLIR ONE and a FLIR SC305 infrared camera. They calculated the sensitivity and specificity of FLIR ONE detected temperature differences that indicate a risk for ulcers using the temperature readings obtained by the FLIR SC305 as gold standard. However, there is no information whether existing ulcers coincided with temperature differences above the threshold, thus an information on the diagnostic accuracy of temperature for the clinical picture of foot ulcers is not available.

Plastic and reconstructive surgery

Traditionally, thermal imaging has two main applications in plastic and reconstructive surgery. One is the assessment of flap tissue viability, and the other the detection of perforating vessels.

A study from Ukraine used the FLIR ONE to assess the viability of skin flaps prepared by the application of an expander for tissue enlargement. While the covered defects at the scalp healed successfully, criteria of thermal imaging indicating tissue viability were not reported [28].

Meyer and co-workers assessed the viability of microvascular free flaps based on the difference (dT) between a reference temperature and the mean temperature of 4 spot measurements in all quadrants of the flap [29]. Prior to anastomosis, flaps appeared intraoperatively to be on average by 6.4 °C cooler. After anastomosis dT averaged between -0.17 and 0.06 °C in 20 patients. One flap was inadequately perfused which was indicated by a decrease in temperature by 2.4°C compared to the reference.

A 93% sensitivity and 96% specificity of thermal imaging for flap perfusion failure was reported in the abstract of an article from Mexico [30]. Since details and criteria of assessing flap viability were not reported in the abstract and the full version of the article could not be retrieved, the evidence raised by this study cannot be determined. In this study flap monitoring was based on a very tight schedule of thermal image recording. On average 60 thermal images were recorded in each of 40 patients, 24 in the first 24 postoperative hours, and further 12 on the following day. Viability evaluation was based on temperature differences between the flap and reference tissue, observed in two consecutive images. A cut-off value of 1.15°C lead to the high diagnostic accuracy of poorly perfused flaps as mentioned above.

Detection of perforator vessels

Hardwicke et al. [31] were the first who assessed in a proof-of-concept study patients and healthy volunteers with thermal imaging for (1) detecting and mapping perforators, (2) defining perforasomes, and (3) monitoring free flaps. The methods described in this article elicited rapidly comments from Norway [32], Hong Kong [33], England [34] and Thailand [35], however, many researchers since followed the concept of employing low-cost thermal camera for perforator detection.

A study from Pakistan investigated in a sample of 184 patients undergoing pedicled or free perforator flap reconstructive surgery, the diagnostic accuracy of perforator detection by thermal imaging using preoperative hand-held ultrasound Doppler as the gold standard [36]. The diagnostic accuracy was found to be 85.9% with a sensitivity of 86.2%, a specificity of 80%. However, thermal characteristics of perforators were not defined. A case report from India reported the potential of the FLIR ONE to provide information on the location of perforators instead of a malfunctioning ultrasound device [37].

Pereira et al. conducted in Chile a concordance study of diagnostic tests in patients who underwent limb reconstruction in 2016 [38]. The authors compared the location of perforators identified in computed tomographic angiographic images of the thigh, and as hotspots in thermal images obtained by the FLIR ONE camera, in relation to their distance from the anterior superior iliac spine. 20 patients were studied including 38 anterolateral thigh flap territories in total, and 117 perforators were identified by computed tomographic angiography and 120 hotspots by thermography. The mean difference in distance was 2.37 mm, with both measurements being obtained within a radius of 20 mm resulting in a concordance kappa index of 0.975. Thermal imaging showed a 100 % sensitivity of and a 98% specificity in detecting perforators.

A study from Denmark compared the detection rate of arterial perforators obtained by the FLIR ONE Pro and the high-end infrared camera FLIR A35SC[39]. The authors examined 23 thighs in 13 healthy volunteers and identified a total of 779 hotspots using both cameras. The A35SC identified on average 33.5 hotspots per thigh, and the FLIR ONE Pro detected identified on average 31.5 hotspots per

thigh. Hot spots were verified by hand-held Doppler and Colour Doppler Ultrasound devices. Both ultrasound devices confirmed in approximately 95% of hot spots detected with either infrared camera a typical signal of perforating arteries.

Chen et al. investigated the value of the FLIR ONE camera in the mapping of the peroneal artery perforators in comparison CT angiography and intraoperative findings [41]. The authors were aware of different behavior of spot temperatures and differentiated between hotspots and slow rewarming spots, but used a questionable e discrimination procedures which was based on normalised temperatures. Thermal imaging detected 42 of the 57 dominant perforators in 24 limbs, resulting in an sensitivity of 74 %.

Vascular disorders

The FLIR ONE was applied in assessment of various vascular disorders including Raynaud`s phenomenon [42, 43, 44], varicose veins [45], monitoring vascular surgery [45, 46, 47, 48, 49] and normobaric hypoxia [50]. While the abstracts of Dakin [42] and Taylor [43] do not reflect the content of their article, the multicentre evaluation of the validity and reliability of responses to hand cold challenge as measured by laser speckle contrast imaging(LSCI) and thermography as an outcome measure for Raynaud's phenomenon [44] contributed a lot to the value of assessment by the FLIR ONE.

In this study, the behaviour of recovering finger temperature after cold water immersion was analysed with standard infrared cameras and a FLIR ONE and compared to LSC-images. Despite the limited facilities of settings for image capture and evaluation of the FLIR ONE, the test-retest reliability of the distal dorsal dif- ference (DDD) and of the reperfusion/rewarming AUC were not significantly different between the three imaging techniques. High convergent validity was found between standard thermography and the FLIR ONE with latent correlation coefficients of 0.9 for DDD and 0.98 for rewarming. Validity of LSCI for standard thermography was 0.65 for DDD and 0.94 for reperfusion/rewarming. It seems there- fore, that rewarming of fingers after cold challenge can be reliably evaluated with a FLIR ONE when standard procedures for image capture and evaluation are strictly followed.

Lin and Sains reported clinical variables of eight patients undergoing endovascular or surgical revascularization confirmed by improvements in thermal images recorded with a FLIR ONE [46]. However, a definition of an improved thermal image was not provided.

The surgical treatment of testicular torsion in a 5-year-old patient was documented by a FLIR ONE [47]. The temperature of the twisted testicle immediately after opening the tunica vaginalis was 31.5°C. 30 seconds after correcting the torsion, the temperature increased to 34.3°C indicating undisturbed testicular perfusion.

Al Shakarchi conducted a prospective cohort study with 25 patients to predict infra inguinal bypass outcome in the immediate post-operative period on basis of thermal images recorded with a FLIR ONE [48]. Spot temperatures were obtained in the posterior tibial, anterior tibial and peroneal angiosome of the foot, the temperature difference between the operated and the contralateral extremity was used to conclude on patent bypass. Thermal findings were compared to the results of hand-held ultrasound Doppler examination. Bypass occlusion occurred in 6/25 patients. 17 patients presented with a warmer foot on the operated side and none of them developed bypass occlusion, but 6 of 8 patients with a colder foot postoperatively lost their bypass patency.

A prospective cohort study was conducted in 100 consecutive patients with chronic kidney disease who had arteriovenous fistula (AVF) formation to prepare them for haemo- dialysis [49]. Infrared thermal imaging was undertaken pre- and post-operatively on the day of surgery to predict clinical patency and functional maturation of AVFs. For evaluation, spot temperature at tip of the middle finger of both hands were measured and the temperature difference between AVF hand and the contralateral hand was defined. Post-operative fistula assessment was performed at 6 weeks after creation and patency was based on clinical assessment of the anastomosis and a AVF width >6mm as measured by ultrasound. Functional maturation as defined by successful successive catheter-free dialysis with two needles. Primary clinical patency was achieved in 70 patients. For 22 patients, whose relative distal temperature remained the same or increased post-operatively, only 3 (14%) achieved fistula clinical patency, compared to 88% of the 76 patients with a drop in relative temperature.

Jones et al. used the FLIR ONE to record the finger temperature during exposure to graded normobaric hypoxia [50]. As expected, increasing levels of hypoxia resulted in decreased blood oxygen saturation that was paralelled by a drop in skin temperature most marked at the nail bed. Returning to the baseline fraction of inspired oxygen lead to rewarming of acral temperatures.

Other medical applications

Anzengruber et al. evaluated the patch testing of contact allergens by thermal imaging using a FLIR ONE and aimed to find possible correlation between the intensity of the patch test response and temperature change [51]. An independent physician who was not part of the study team evaluated clinically the lesions as "negative", "irritant", "allergic (+, ++, +++)". Only 420 positive lesions in 129 patients were considered and served as gold standard for the thermographic evaluation, which was based on the difference of spot temperatures within the area of the skin response and the adjacent not tested skin. The mean change of temperature (Δt) of irritant skin was 0.17 °C ± 0.31 Patch tests classified as allergic reactions were warmer (mean Δt = 0.72 °C ±0.67).

Table 4
Clinical studies

Author (Publication year)	Research aim	Study type/participants	Comparative Assessment	Temperature measurement	Result
Al Shakarchi et al. (2017}	Patency of arteriovenous fistula after recent formation	Prospective cohort study with 100 patients prepared for haemodialysis	Clinical assessment AVF width measured by ultrasound	Spot temperature at tip of the middle finger of both hands Temperature difference between AVF hand and the contralateral hand	Clinical primary patency was achieved in 70 patients. For 22 patients, whose relative distal temperature remained the same or increased post-operatively, only 3 (14%) achieved fistula clinical patency, compared to 88% of the 76 patients with a drop in relative temperature
Al Shakarchi et al.. (2019)	Prediction of bypass patency from thermal imaging in the immediate post-operative period	Prospective cohort study with 25 patients	Hand-held Doppler ultrasound	Spot temperatures in the foot angiosomes, 1: Posterior Tibial, 2: Anterior Tibial, 3: Peroneal. Temperature difference between the operated and the contralateral extremity.	Bypass occlusion occurred in 6/25 patients. 17 patients presented with a warmer foot on the operated side and none of them developed bypass occlusion, but6 of 8 patients with a colder foot postoperatively lost their bypass patency.
Anzengruber et al. (2019)	Evaluation of patch testing of contact allergens by thermal imaging, possible correlation between the intensity of the patch test response and temperature change	420 positive lesions in 129 patients	An independent physician (who was not part of the study team) clinically evaluated the lesion (negative, irritant, allergic +, ++, +++)	Difference of spot temperatures within the area of the skin response and the adjacent not tested skin.	The mean change of temperature (Dt) of irritant skin was 0.17 °C ± 0.31 Patch tests classified as allergic reactions were warmer (mean Dt = 0.72 °C ±0.67)
Ganon et al (2020)	Prediction of time for skin burn healing in children	Prospective cohort study with 40 children	Clinical burn assessment at day15 of therapy Not healed =deep burns presenting <95% of epithelialized wound surface or have been grafted Healed=superficial burns that healed before day 15.	Difference between the spot temperature recorded at the centre of the wound and the temperature of unaffected skin 3cm apart from the wound edge or on the contralateral limb. Thermal imaging was performed three times T1: day 1 to day 3 after burn, T2: day 4 to day 7, - T3: day 8 to day 10.	The mean ΔT at T1, T2 and T3 in the group of non-healed burns are -3.6 °C, -0.67 °C and -1.76 “C respectively. In the group with healed wounds, these values are respectively -1.1 °C, 1.51 °C and 2.24 °C. ROC-analysis revealed for T3 at a threshold of -1,2°C an AUC of 0.968, related to sensitivity of 56.7% and a specificity of 100%.
Carrière et al. (2020)	Prediction of LDI based probability of skin burn healing, in less than 14 days, between 14 and 21 days, and more than 21 days.	Prospective cohort study with 32 patients	Laser Doppler Imaging (LDI)	Difference between the mean value of 4 spot temperatures recorded at defined sites within the wound area and the temperature of a circular reference area in unaffected skin at least 3cm apart from the wound edge. Imaging was performed between 2 and 5 days postburn.	ÄT cutoff values of 0.6°C (sensitivity 68%, specificity 95%) and -2.3°C (sensitivity 30%, specificity 95%) discriminated between burn wounds with the LDI based potential to heal in <14 and =14 days, and burn wound that heal in =21 and>21 days, respectively.
Jaspers et al. (2017)	Prediction of time for skin burn healing	Prospective cohort study with 41 patients (50 wounds)	The day of healing was defined as the post-burn day when at least 95% of the studied wound was epithelialised. 3 healing categories: (I) 14 days, (II) 15–21 days and (III) >21 days, considering the day of the injury as 0.	Mean temperature in circular ROI at the centre of the wound, mean temperature of circular reference ROI located in unaffected skin, at least 3cm apart from the wound edge or on the contralateral limb. Difference between both ROIs. Thermal imaging was performed at T1: day 1 to day 3 after burn, T2: day 4 to day 7; T3:day 8 to day 10	ROC analysis obtained an AUC of 0.69 representing a sensitivity of 46% and specificity of 82% at the optimal cut-off point of -1.15°C.

Table 4
Clinical studies continued

Author (Publication year)	Research aim	Study type/participants	Comparative Assessment	Temperature measurement	Result
Bouallal et al (2020)	Comparison of the plantar foot temperature in diabetics with different risk to develop foot complications	Cross-sectional observation study in 122 diabetics Low risk: 52 patients medium risk: 26 patients high risk: 44 patients	Foot temperatures between risk groups	Plantar foot temperatures before and after cold stress, pixelwise temperature difference between right and left sole,	Significant differences of temperatures between the 3 groups based on Student t-test.
Meyer et al. (2020)	Evaluation of the utility of a low-cost thermal imaging device for monitoring microvascular free flaps used in head and neck reconstruction	Prospective cohort study with 21 patients	Clinical assessment including pinprick with a 25-gauge needle or with an implantable Cook-Swartz Doppler probe or a handheld Doppler probe.	The average flap temperature was calculated as the mean of four temperature points, one in each quadrant of the flap. This was compared to the average surrounding tissue temperature (mean of four temperature points) to obtain the difference in temperature between the flap and surrounding tissue (dT). Thermal imaging was performed prior to incision at the start of case (FS), after the flap was raised but prior to dividing the pedicle (FPr), ischemic prior to re-anastomosis (FI), and 30 minutes or more after re-anastomosis (FPo). Postoperatively, thermal images were taken of the flap twice daily, approximately every 12 hours, for up to seven days (1-7 a or p, for postoperative day and am or pm)	The mean dT for flaps intraoperatively prior to anastomosis was -11.47 °F. For 20 patients, dT averaged between -0.30 to 0.12 °F. One flap was inadequately perfused and dT was found to be -4.35 °F.
van Doremalen et al. (2019)	Diagnostic accuracy of FLIR-ONE to detect temperature differences beyond the diagnostic threshold for ulcer detection as was obtained by the FLIR SC305 camera	Cross-sectional observation study in 32 patients (diabetic) neuropathy	Number of cases with a temperature difference >1.35°C in the total foot or >2.2°C between two pre-specified contralateral regions as detected with both infrared cameras	Mean temperature of the total area of the plantar foot, mean temperature in each of nine pre-specified circular ROIs	For the total foot, the sensitivity was 94% and specificity was 86%. For all nine regions on the plantar foot combined, 93% sensitivity and 91% specificity were obtained.
Hennessy et al. (2020)	Comparison of the rate of perforator detection by CTA, Doppler ultrasound (US), and thermal imaging mapping in DIEAP flaps	Prospective cohort study with 13 women undergoing breast reconstruction	Number and location of CTA, ultrasound, and thermal signals on the flap area	"Hot spots" Not further defined	40 (57%) out of 70 perforators identified by Doppler US showed a corresponding hot spot on the thermal image 58 (69%) out of 84 perforators identified by CTA showed a corresponding hot spot on the thermal image
Chen et al. (2018)	To investigate the value of a smartphone compatible thermal imaging camera in the mapping of the peroneal artery perforators	Prospective cohort study with 12 patients	CT angiography; intraoperative findings.	Differentiation between hotspots and slow rewarming spots was based on normalised temperatures	Thermal imaging detected 42 of the 57 dominant perforators in 24 limbs.

Table 5
Reported method of thermal imaging

Author (Publication year)	Ambient temperature	Camera	Distance to target/image content	evaluation	Tool for temperature measurement	Compared to other assessment
Al Shakarchi et al.(2017)	Not reported	FLIR ONE, held in hands	Both forearms and hands within the image	quantitatively	Spot meter	Clinically ultrasound
Al Shakarchi et al.(2019)	Not reported (bedside at the ward)	FLIR ONE Pro, held in hands	Both feet (anterior view: from 2 cm above the ankle to the toes; plantar view: both soles) within the image.	quantitatively	FLIR ONE app	Clinically, rate of graft occlusion
Anzengruber et al. (2019)	stable at 21°C	FLIR ONE attached to an iPhone, vertically held in hands	Approximately 20 cm away from the skin	quantitatively	FLIR ONE app (Version 20.52).	Visual evaluation, relationship between temperature and grade of response
Ganon et al. (2020)	19 ± 0.2 °C	FLIR ONE attached to an Asus tablet, held in hands	Burn area within the image	quantitatively	FLIR One app	Healed/not healed on day 15
Carrière et al (2020)	Not reported	FLIR ONE Pro attached to an iPad mini, held in hands	The burn wound of interest and a reference area of healthy skin were within the image	quantitatively	FLIR One app	LDI derived blood flow rate, with 3 classes of potential healing within defined periods.
Jaspers et al. (2017)	Outpatient clinic 23.3°C(21.2–26.9) Burn center 23.4°C(19.8–24.8)	FLIR ONE Gen 2 attached to an iPad mini, held in hands	0.5 to 1m The burn wound of interest and a reference area of healthy skin were within the image	quantitatively	FLIR Tools	Healed/not healed on day 21
Bouallal et al (2020	Room temperature not reported, Water bath 15°C for 1 minute	FLIR ONE Pro attached to a Samsung galaxy S8, held in hands	Segmented foot soles of the patients who sat on a chair with a stool supporting their legs in full knee extension.	quantitatively	Self-designed software for image segmentation, temperature readings and pixelwise temperature difference between right and left sole	Temperature comparisons between the 3 risk groups
van Doremalen et al. (2019)	Not reported, (images captured in the outpatient clinic)	FLIR ONE Gen 2 attached to Motorola XT1642 Moto G4 Plus smartphone held in handFLIR SC305 combined to a Canon EOS 40D, mounted in a wooden box	FLIR SC305 combined to a Canon EOS 40D, mounted in a wooden box	quantitatively	FLIR ONE app (by Georg Friederich) costum made Matlab software for FLIR SC305	Detection rate of pre-defined temperature thresholds indicating a high risk for ulcers
Hennessy et al. (2020)	22°C	FLIR ONE	0.5m	qualitatively	FLIR One app	computed tomography angiography (CTA Doppler ultrasound
Meyer et al. (2020)	Not reported	FLIR ONE Gen 2 attached to an iPhone 6, heldd in hands	0.3m	quantitatively	Not reported, but FLIR One app is likely	Clinical assessment of flap viability
Chen et al. (2018)	26°C	FLIR ONE PRO attached to an iPad, mounted on a tripod	0.4m	quantitatively	FLIR Tools	computed tomography angiography (CTA) intraoperative inspection

Li et al. compared the accuracy of the ALT-70 predictive model and thermal imaging in diagnosing lower extremity cellulitis [52]. A FLIR ONE Gen 2 was used to acquire skin temperatures corresponding to the warmest area of the affected and (contralateral) sites of the lower extremities. A temperature difference of ≥0.47°C and an ALT-70 score ≥3 points and the combined criteria of thermography and ALT-70 were used to calculate the diagnostic accuracy in relation to the clinical diagnosis of cellulitis as gold standard. Both sensitivity and specificity were higher for ALT-70 than for thermography, but the combined criteria achieved the highest diagnostic accuracy with a sensitivity of 84.8% and a specificity of 71.4%.

A Dutch study compared FLIR ONE Pro thermal images to the cold sensation test (CST) as indicator of successful epidural anaesthesia [53]. Thermal images were taken of the abdomen and the thighs of the supine patient in a non-perpendicular, angled view at 5, 10 and 15 minutes after administration of epidural anaesthesia. Thermal images were evaluated quantitatively and after image storage quantitatively, but the procedures of temperature measurement were not reported. An ice cube was used to perform the cold sensation test after recording the third thermogram. A cold sensation test was scored positive when cold perception was absent in the blocked dermatomes, and negative when a perception of cold existed. In patients with a successful block a temperature drop was observed after 10 min following epidural anaesthesia and this drop remained for further 5 minutes. In patients with an unsuccessful block, there was an initial drop in temperature, there was an initial drop in temperature that returned to baseline temperature at 15 min following epidural anaesthesia. Successful epidural anaesthesia was defined as a Numeric Rating Scale (NRS) score for pain≤4 measured immediately after surgery. The NRS was used as gold standard for defining the diagnostic accuracy of thermography and cold sensation testing. The diagnostic accuracy of thermal imaging and cold sensations testing was similar, with higher sensitivity for CST (0.97 vs.0.54 thermal imaging) and higher specificity for thermal imaging (0.67 vs.0.25 CST).

A conference paper from Korea was primarily focused on image processing of breast thermograms recorded with a FLIR A320 and a FLIR ONE iOS [54]. There was a slightly better automatic detection of ROIs in images recorded with the FLIR A320 than with the smartphone based infrared camera. Due to the study design, no information was obtained on the value of FLIR ONE in breast cancer diagnosis.

A paper from Peru claimed to show the effects of heating the muscles of sportsmen by using a FLIR ONE Pro Android [55]. However, it remains unclear if passive heating was applied or just warming-up exercises have performed.

Della Corte recorded with a FLIR ONE Pro iOS skin temperatures on the anterior thigh of recreational athletes after resistance training of the dominant leg at an intensity equal to 70% of 10 repetition maximum [56]. Thigh temperatures prior and post exercise were not significantly different neither on the exercising side nor on the contralateral leg. The study was performed under strictly controlled conditions, but the automatically selected temperature window of the infrared camera resulted in different temperature endpoints of the colour bar that makes visual comparison of thermal images difficult.

In another study, Della Corte described skin temperature changes after a single session of resistance training of different workload, again recorded by the FLIR ONE Pro iOS camera. The participants performed three sets of maximal repetitions (up to concentric failure) in the leg extension exercise with loads of 60% (power training protocol -PTP) and 90% (strength training protocol - STP) of 1 repetition maximum (RM). respectively. Thermal Imaging and vertical countermovement jumps were performed before and after the training session. There were increases by ~5 degree in both mean maximum and mean minimum skin temperature of after the PTP training, also a reduction of jump height. The temperature changes were much smaller (approximately 2.8°C) after STP training, but jump height increased slightly by 0.6 cm, although the jump height prior to STP training was 4cm less than the height before PTP training.

Robinson and colleagues recorded with a FLIR ONE PRo camera temperature changes of the burr used for osteotomy in foot surgery [59]. The temperature generated during the procedure was found to be significantly associated with the burr diameter used but was not affected by the type of motor. The highest mean of burr temperature was 36 ± 5°C with a corresponding temperature in adjacent tissue of 29 ± 1°C.

A conference paper from China announced a FLIR ONE Pro based device for screening of respiratory disease [60]. But only the concept of such a device and preliminary report of successful functioning were provided, but experimental data were not given.

FLIR ONE cameras were used to obtain the surface temperature of the eye [61,62], for monitoring heat production during teeth preparation [63] and for mass fever screening [64]. The exceptional high eye temperatures between 37.2 and 40.1 reported in [62] for patients with active Graves' ophthalmopathy, raise questions on the accuracy of the temperature measurements and the thermo-physiological background of the authors and the editor of the journal, who published these data without any comment.

In veterinary medicine, the FLIR ONE was used in equine medicine [65] and in zoo animals, particularly birds, to detect signs of inflammation [66]. However, the performance of the FLIR ONE does not meet the minimal requirements proposed by the American Academy of Thermology for animal thermography [66].

Animal experiments

FLIR ONE cameras were used for thermal assessment in a mouse model of fatty liver disease [67] and of cardiac remodelling [68], respectively. Han et al. compared in a rat perforator flap model the potential of indocyanine green angiography, near-infrared spectroscopy derived tissue oximetry, and thermal imaging to predict tissue necrosis [69]. Indocyanine green angiography performed best in predicting flap necrosis in this study, but tissue oximetry and thermal imaging were also capable of predicting necrosis.

Hummelink and co-workers studied in a porcine model the potential of the FLIR ONE in the detection of failing free flaps during post-operative monitoring [70]. Free myo-cutaneous rectus abdominis flaps were harvested in 16 female landrace pigs and replanted after several hours of storage. All flaps were assessed with indocyanine green fluorescence angiography as well as hourly clinical assessment of skin colour, turgor, and capillary refill. In addition, visual and thermal images were taken simultaneously with a FLIR One Gen 2. A Matlab based software was used to convert the thermal image into numerical value, register the thermal image to the photograph and calculate temperatures for the flap and the reference area. The surface temperature of the replanted flap was compared to the reference skin, and the temperature difference of the free flap calculated over time. Out of 16 flaps, three flaps failed due to arterial failure and one flap developed venous congestion. All unsuccessful flaps showed lower temperatures after failure compared to the uncompromised free flaps.

Two studies investigated cardiovascular circulation with the FLIR ONE in animal models. Barron et co-workers studied in 10 swine limb perfusion and tourniquet effectiveness under normal and haemorrhagic conditions with 40% loss of total blood volume [70]. Three experiments were conducted: experiment 1 simulated proper tourniquet application, experiment 2 had one of two tourniquets inadequately tightened, and experiment 3 had one of two tourniquets inadequately tightened while simulating blackout-combat conditions. Static thermal images were taken at multiple time points up to 30 minutes. Thermal images were then presented to blinded evaluators who assessed adequacy of tourniquet placement. The temperature readings from thermal images decreased significantly after proper tourniquet placement in all animals, with no difference between haemorrhaged and non-haemorrhaged groups at 30 minutes. Qualitative thermal image analysis showed clearly visible temperature differences in all animals between baseline, adequate tourniquet, and inadequate tourniquet irrespective to circulating blood volume. 55 out of 62 blinded evaluators correctly identified adequate and inadequate tourniquet placement at 5 minutes.

Sokol et al. investigated in 6 swine the effects of the resuscitative endovascular balloon occlusion of the aorta on the surface temperature at five anatomic points (axilla [A], subcostal [S], umbilical [U], inguinal [I], medial malleolar [M]), recorded with a FLIR ONE [71]. The authors based their evaluation on temperature ratios, with best prediction of occlusion for the ratio S/M. Since temperature as an interval scaled quantity, the formation of a ratio is regarded as an inappropriate method of evaluation.

Reporting of measurement conditions

6 of 11 selected clinical papers listed in table 5 did not report ambient temperature, while all but one articles reporting camera performance provided information on room temperature (table 3). All articles reported the distance from the camera to the target and/or the content of the field of view. The FLIR ONE model was identified unambiguously in 12/16 articles. For image capture, the device was mounted to a tripod in 3 studies, held in hand in 11 studies, and camera fixation was unclear in the remaining 2 investigations. In all articles, there was information on form and position of ROIs, the extracted temperature variable and the software used for temperature readings. Information on comparative assessments was also available.

Discussion

The hype in smartphone based infrared cameras has already arrived in medicine, where an increasing number of new medical applications is now published. The current publications may be classified in projects, wishful thinking based promotional material, case reports, reports on the performance assessment of the device, and well-planned and well-conducted clinical trials. Since the measurement performance of the FLIR ONE camera is far from excellence [1, 3, 65] it is not surprising that applications which function very well with qualitative to semiquantitative evaluation of the thermal image achieve favourable results with the FLIR One [38,39,48,49]. Relative temperatures such as the side-to-side difference in temperature of corresponding regions of interest or the temperature difference between wound area and unaffected skin can also be reliably measured [2,10]. Strictly following standard procedures for infrared imaging can remove other sources of measurement uncertainty not related to the camera performance [44, 65].

The FLIR ONE may have a place for quick documentation of unexpected thermal phenomena [37,47]. When used as pictorial documentation, it is important to take images always in the same temperature window. Allowing that the temperature window is automatically selected by the temperature scene, leads to the fact, that the same colour indicate different temperature levels. Novices in the application of thermal imaging, should also remember that human skin temperature exceeds the value of 37.0 °C only in the case of fever or severe exertional hyperthermia. In all other conditions, a skin temperature higher than 37.0 C° might be caused by an external heat source pointing to the skin or most likely a measurement failure of the device. In the evaluation of temperature readings, the rules of statistics must not be infringed. It is most important to remember, that the temperature unit °C indicates an interval scaled quantity, of

which a ratio (=temperature/temperature) must not be defined. Consequently, normalised temperatures [41] or temperature percentages [57] are meaningless constructs.

It is admitted that the price for a FLIR ONE is extremely attractive. However, the thermal information you can get is similar to that derived from liquid crystal contact thermography or commercial infrared camera produced in the 1980ties, when spot temperature measurements become established in the evaluation software of that time. However, using the FLIR One in combination with a strict protocol, can improve the performance of the camera, in trade-off to the flexibility and spontaneity of its application. It is possible to use the FLIR ONE in a pilot study. However, if accurate and reliable temperature measurements are needed, the low-cost camera will quickly be identified as the weakest link in the whole project.

References

1.Vardasca R, Magalhaes C, Silva P, Kluwe B, Mendes J. Are the IR cameras FLIR ONE suitable for clinical applications? Thermo-logy International 2019; 29 (3): 95-102.

2.Alfieri FM, da Silva Dias C, de Oliveira Vargas e Silva NC, dos Santos ACA, Battistella LR. Comparison of iOS smartphone-attached infrared camera and conventional FLIR camera for human temperature measurement: An agreement study. Thermology International 2020; 30 (3): 91-96.

3.Curran A, Klein M, Hepokoski M, Packard C. Improving the accuracy of infrared measurements of skin temperature. Extreme Physiology & Medicine 2015; 4 (Suppl 1): A140

4.Villa E, Arteaga-Marrero N, Ruiz-Alzola J. Performance Assessment of Low-Cost Thermal Cameras for Medical Applications. Sensors 2020, 20(5), 1321

5.Wang SC, Anderson JAE, Evans R, Woo K, Beland B, Sasseville D, Moreau L. Point-of-care wound visioning technology: Reproducibility and accuracy of a wound measurement app. PLoS ONE 2017; 12 (8): e0183139.

6.Cao J, Currie K, Carry P, Maddox G, Nino S, Ipaktchi K. Smartphone-based thermal imaging: A new modality for tissue temperature measurement in hand and upper extremity surgeries. Hand 2018, 13(3), 350-354.

7.Kanazawa T, Nakagami G, Goto T, Noguchi H, Oe M, Miyagaki T, Hayashi A, Sasaki S, Sanada H. Use of smartphone attached mobile thermography assessing subclinical inflammation: A pilot study. Journal of Wound Care 2016; 25 (4): 177-182.

8.Rafferty J, Cleland I, Nugent C, Armstrong K, Madill G. An evaluation of contactless thermal sensing elements for use in a technology based diabetic foot disease detection solution. In: The 38th Annual International Conference of the IEEE Engineering in Medicine and Biology Society. 2016

9. van Doremalen RFM, van Netten JJ, van Baal JG, Vollenbroek-Hutten MMR, van der Heijden F. Validation of low-cost smartphone-based thermal camera for diabetic foot assessment. Diabetes Research and Clinical Practice 2019; 149;132-139

10. Jaspers MEH, Carrière ME, Meij-de Vries A, Klaessens JHGM, van Zuijlen PPM. The FLIR ONE thermal imager for the assessment of burn wounds: Reliability and validity study. Burns 2017; 43 (7): 1516-1523

11. Oliver B, Munro A, Gerald S, Herrington L. The reliability of an achilles tendon infrared image analysis method. Thermology International 2019; 29 (4): 136-145.

12. Oliver B, Munro A, Herrington L. The effect of distance and angle of a smartphone-compatible infrared thermal imaging camera on skin temperature at the midportion of the Achilles tendon. Thermology International 2020; 30 (2): 51-57.

13. Vlig M, Boekema BKHL, Ulrich MMW. Porcine models. In: Garcia-Galeta E, ed, Biomaterials for Skin Repair and Regeneration. Cambridge: Woodhead Publishing 2019; pp.297-330.

14. Fraiwan L, Al Khodari M, Ninan J, Mustafa B, Saleh A, Ghazal M. Diabetic foot ulcer mobile detection system using smart phone thermal camera: A feasibility study. BioMedical Engineering Online 2017; 16 (1): 117.

15.Fraiwan L, Ninan J, Al-Khodari M. Mobile application for ulcer detection. Open Biomedical Engineering Journal 2018; 12 (1): 16-26.

16.Quinn S, Saunders C, Cleland I, Nugent C, Garcia- Constantino M, Cundell J, Madill G, Morrison G. A Thermal Imaging Solution for Early Detection of Pre-ulcerative Diabetic Hotspots. Proceedings of the Annual International Conference of the IEEE Engineering in Medicine and Biology Society EMBS 2019; 8856900: 1737-1740.

17. Diaz C, Garcia-Zapirain B, Castillo C, Sierra-Sosa D, Elmaghraby A, Kim PJ. Simulation and development of a system for the analysis of pressure ulcers. 2017 IEEE International Symposium on Signal Processing and Information Technology ISSPIT 2018; pp, 453-458.

18.Marina CN, Raducu L, Ardeleanu V, Florescu IP, Jecan CR. Thermographic camera in traumatology diabetic foot and reconstructive procedures. Injury 2020; Mar. DOI: 10.1016/j.injury.2020.03.020

19.Shamloul N, Ghias MH, Khachemoune A. The Utility of Smartphone Applications and Technology in Wound Healing. International Journal of Lower Extremity Wounds 2019; 18 (3): 228-235

20.Xue EY, Chandler LK, Viviano SL, Keith JD. Use of FLIR ONE Smartphone Thermography in Burn Wound Assessment. Annals of Plastic Surgery 2018; 80 (4): S236-S238.

21.Maddah E, Beigzadeh B. Use of a smartphone thermometer to monitor thermal conductivity changes in diabetic foot ulcers: A pilot study. Journal of Wound Care 2020; 29 (1): 61-66

22.Ganon S, Guédon A, Cassier S, Atlan M. Contribution of thermal imaging in determining the depth of pediatric acute burns. Burns 2020; 46 (5): 1091-1099.

23.Carrière ME, de Haas LEM, Pijpe A, Meij-de Vries A, Gardien KLM, van Zuijlen PPM, Jaspers MEH. Validity of thermography for measuring burn wound healing potential. Wound Repair and Regeneration 2020; 28 (3): 347-354.

24.Nischwitz SP, Luze H, Kamolz L-P. Thermal imaging via FLIR One - A promising tool in clinical burn care and research. Burns 2020; 46 (4): 988-989.

25.Boguski R, Khan T, Woelfel S, D'Huyvetter K, Armstrong AA, Armstrong DG. Clinical utility of mobile phone-based thermography and low-cost infrared handheld thermometry in high-risk diabetic foot. Indian Journal of Vascular and Endovascular Surgery 2019, 6(1), 7.

26. Meneses-Claudio B, Alvarado-Díaz W, Flores-Medina F, Vargas-Cuentas NI, Roman-Gonzalez A. Detection of suspicious of diabetic feet using thermal image. International Journal of Advanced Computer Science and Applications 2019; 10 (6): 379-383.

27. Bouallal D, Bougrine A, Douzi H, Harba R, Canals R, Vilcahuaman L, Arbanil H. Segmentation of plantar foot thermal images: Application to diabetic foot diagnosis. In: Proceedings of the 2020 International Conference on Systems Signals and Image Processing (IWSSIP). 2020; art, no, 9145167: 116-121

28.Abdullaiev R, Oleynik G, Kremen V, Gryazin A, Timchenko E. Improvement of the dermatension method in the reconstructive-recovery surgery of defects of soft tissues of various etiology. Georgian Medical News 2018; (283): 7-10.

29.Meyer A, Roof S, Gray ML, Fan CJ, Barber B, Miles BA, Teng M, Genden E, Rosenberg JD. Thermal imaging for microvascular free tissue transfer monitoring: Feasibility study using a low cost commercially available mobile phone imaging system. Head and Neck 2020; 42 (10): 2941-2947.

30.Cruz-Segura A, Cruz-Domínguez MP, Jara LJ, Miliar-García Á, Hernández-Soler A, Grajeda-López P, Martínez-Bencomo MA, Montes-Cortés DH. Early Detection of Vascular Obstruction in Microvascular Flaps Using a Thermographic Camera. Journal of Reconstructive Microsurgery 2019; 35 (7): 541-548.

31.Hardwicke JT, Osmani O, Skillman JM. Detection of perforators using smartphone thermal imaging. Plastic and Reconstructive Surgery 2016; 137 (1): 39-41.

32.Weum S, Lott A, de Weerd L. Detection of Perforators Using Smartphone Thermal Imaging. Plastic and Reconstructive Surgery 2016, 138(5), 938e-940e

33.Ko WS, Chiu T. Detection of perforators using smartphone thermal imaging. Plastic and Reconstructive Surgery 2016, 138(2) 380e-381e

34.Konczalik W, Nikkhah D, Mosahebi A. Applications of Smartphone thermal camera imaging system in monitoring of the deep inferior epigastric perforator flap for breast reconstruction. Microsurgery 2017; 37 (5): 457-458

35.Suphachokauychai S, Kiranantawat K, Sananpanic K. Detection of perforators using smartphone thermal imaging. Plastic and Reconstructive Surgery Global Open 2016; 4(5) e722.

36.Patel SS, Homsy C, Atamian EK, Chaffin AE. Thermal Imaging Facilitates Design of a Keystone Perforator Island Flap for a Myxofibrosarcoma Resection Reconstruction: Case Report. Plastic and Reconstructive Surgery - Global Open 2019; 7 (8): e2359

37.Rabbani MJ, Ilyas A, Rabbani A, Ul Abidin Z, Tarar MN. Accuracy of thermal imaging camera in identification of perforators. Journal of the College of Physicians and Surgeons Pakistan 2020; 30 (5): 512-515

38.Pereira N, Valenzuela D, Mangelsdorff G, Kufeke M, Roa R. Detection of perforators for free flap planning using smartphone thermal imaging: A concordance study with computed tomographic angiography in 120 perforators. Plastic and Reconstructive Surgery 2018; 141 (3): 787-792.

39.Obinah MPB, Nielsen M, Hölmich LR. High-end versus Low-end Thermal Imaging for Detection of Arterial Perforators. Plastic and Reconstructive surgery. Global Open 2020, 8(10), e3175-e3175.

40.Hennessy O, McLoughlin R, McInerney N, Hussey A, Potter S. Smartphone thermal imaging for preoperative perforator mapping in DIEP flap breast reconstruction. European Journal of Plastic Surgery 2020; 43:743-750

41.Chen R, Huang Z-Q, Chen W-L, Ou Z-P, Li S-H, Wang J-G. Value of a smartphone-compatible thermal imaging camera in the detection of peroneal artery perforators: Comparative study with computed tomography angiography. Head and Neck 2019; 41 (5): 1450-1456.

42.Dakin C. Self-monitoring of Raynaud's phenomenon with FLIR ONE® PRO. Imaging Science Journal 2018; 66 (5): 314-319

43.Taylor I. Customising the cold challenge: Pilot study of an altered Raynaud's phenomena assessment method for data generation. Lecture Notes of the Institute for Computer Sciences Social-Informatics and Telecommunications Engineering LNICST 2017; 192: 115-121.5647.

44.Wilkinson JD, Leggett SA, Marjanovic EJ, Moore TL, Allen J, Anderson ME, Britton J, Buch MH, Del Galdo F, Denton CP, Dinsdale G, Griffiths B, Hall F, Howell K, MacDonald A, McHugh NJ, Manning JB, Pauling JD, Roberts C, Shipley JA, Herrick AL, Murray AK. A Multicenter Study of the Validity and Reliability of Responses to Hand Cold Challenge as Measured by Laser Speckle Contrast Imaging and Thermography: Outcome Measures for Systemic Sclerosis-Related Raynaud's Phenomenon. Arthritis and Rheumatology 2018; 70 (6): 903-911.

45.Meneses-Claudio B, Alvarado-Diaz W, Roman-Gonzalez A. Detection of suspicions of Varicose veins in the legs using thermal imaging. International Journal of Advanced Computer Science and Applications 2019; 10 (5): 431-435.

46.Lin PH, Saines M. Assessment of lower extremity ischemia using smartphone thermographic imaging. Journal of Vascular Surgery Cases and Innovative Techniques 2017; 3 (4): 205-208.

47. Fernandez N, Lorenzo A, Blais A-S, Matava C. Thermographic Patterns for Real-time Intraoperative Monitoring of Testicular Reperfusion following Surgical Testicular Detorsion. Urologia Colombiana 2018; 27 (3): 294-298

48. Al Shakarchi J, Inston N, Dabare D, Newman J, Garnham A, Hobbs S, Wall M. Pilot study on the use of infrared thermal imaging to predict infra inguinal bypass outcome in the immediate post-operative period. Vascular 2019; 27 (6): 663-667

49. Al Shakarchi J, Hodson J, Field M, Inston N. Novel use of infrared thermal imaging to predict arteriovenous fistula patency and maturation. Journal of Vascular Access 2017; 18 (4): 313-31845

50.Jones D, Covins SF, Miller GE, Morrison KI, Clark AG, Calcott SD, Anderson AM, Lucas SJE, Imray CHE. Infrared thermographic analysis of surface temperature of the hands during exposure to normobaric hypoxia. High Altitude Medicine and Biology 2018; 19 (4): 388-393.

51. Anzengruber F, Alotaibi F, Kaufmann LS, Ghosh A, Oswald MR, Maul J-T, Meier B, French LE, Bonmarin M, Navarini AA. Thermography: High sensitivity and specificity diagnosing contact dermatitis in patch testing. Allergology International 2019; 68 (2): 254-258..

52.Li DG, Dewan AK, Xia FD, Khosravi H, Joyce C, Mostaghimi A. The ALT-70 predictive model outperforms thermal imaging for the diagnosis of lower extremity cellulitis: A prospective evaluation. Journal of the American Academy of Dermatology 2018; 79 (6): 1076-1080, e1.

53.Bruins AA, Kistemaker KRJ, Boom A, Klaessens JHGM, Verdaasdonk RM, Boer C. Thermographic skin temperature measurement compared with cold sensation in predicting the efficacy and distribution of epidural anesthesia. Journal of Clinical Monitoring and Computing 2018; 32 (2): 335-341.

54.Min S, Heo J, Kong Y, Nam Y, Ley P, Jung B-K, Oh D, Shin W. Thermal infrared image analysis for breast cancer detection. KSII Transactions on Internet and Information Systems 2017; 11 (2): 1134-1147.65.

55.Meneses-Claudio B, Alvarado-Díaz W, Flores-Medina F, Vargas-Cuentas NI, Roman-Gonzalez A. Muscles heating analysis in sportspeople to prevent muscle injuries using thermal images. International Journal of Advanced Computer Science and Applications 2019; 10 (6): 40-44.

56.Della Corte J, Pinheiro CDB, Lima BLP, Vignoli FDA, De Oliveira JGM, De Castro JBP, Lima VP. Thermographic analysis of thighs of trained men during the leg extension exercise. Journal of Physical Education and Sport 2019; 19 (4): 2458-2465.

57.Della Corte J, Pereira WLM, Corrêa EELS, De Oliveira JGM, Lima BLP, De Castro JBP, Lima VP. Influence of power and maximal strength training on thermal reaction and vertical jump performance in Brazilian basketball players: A preliminary study. Biomedical Human Kinetics 2020; 12 (1): 91-100.

58.Jiang Z, Hu M, Zhai G. Portable health screening device of respiratory infections. 2020 IEEE International Conference on Multimedia and Expo Workshops ICMEW 2020; 9105969.

59Robinson D, Heller E, Yassin M. Comparing the Temperature Effect of Dedicated Minimally Invasive Motor System to the Discontinuous Use of Rotatory Burrs in the Correction of Hallux Valgus. Foot and Ankle Specialist 2019; Dec 2; 1938640019890225

61.Capriotti L, Greco K, Paolone G, Sberna MT, Cantatore G. Removal of fiber posts during endodontic retreatments using ultrasonic tips: A comparison between two different endodontic fiber posts. Giornale Italiano di Endodonzia 2018; 32 (1): 47-50.

62. Riguetto CM, Minicucci WJ, Neto AM, Tambascia MA, Zantut-Wittmann DE. Value of Infrared Thermography Camera Attached to a Smartphone for Evaluation and Follow-up of Patients with Graves' Ophthalmopathy. International Journal of Endocrinology 2019; art, no, 7065713.

63.Zadorozhnyy O. New possibilities of infrared thermography in ophthalmology. Oftalmologija, Vostochnaja Evropa 2019; 9 (2): 184-191.

64.Somboonkaew A, Vuttivong S, Prempree P, Amarit R, Chanhorm S, Chaitavon K, Porntheeraphat S, Sumriddetchkajorn S. Temperature-compensated infrared-based low-cost mobile platform module for mass human temperature screening. Applied Optics 2020; 59 (17): E112-E117.

65.Howell K, Dudek K, Soroko M. Thermal camera performance and image analysis repeatability in equine thermography. 2020; Infrared Physics and Technology 110 art, no, 103447.

66.Huynh M. Smartphone-Based Device in Exotic Pet Medicine. Veterinary Clinics of North America - Exotic Animal Practice 2019; 22 (3): 349-366.

67.Brzezinski RY, Levin-Kotler L, Rabin N, Ovadia-Blechman Z, Zimmer Y, Sternfeld A, Finchelman JM, Unis R, Lewis N, Tepper-Shaihov O, Naftali-Shani N, Balint-Lahat N, Safran M, Ben-Ari Z, Grossman E, Leor J, Hoffer O. Automated thermal imaging for the detection of fatty liver disease. Scientific Reports 2020; 10 (1) art, no, 15532.

68.Brzezinski RY, Ovadia-Blechman Z, Lewis N, Rabin N, Zimmer Y, Levin-Kotler L, Tepper-Shaihov O, Naftali-Shani N,

Tsoref O, Grossman E, Leor J, Hoffer O. Non-invasive thermal imaging of cardiac remodeling in mice. Biomedical Optics Express 2019; 10 (12): 6189-6203.

69.Han T, Khavanin N, Wu J, Zang M, Zhu S, Chen B, Li S, Liu Y, Sacks JM. Indocyanine green angiography predicts tissue necrosis more accurately than thermal imaging and near-infrared spectroscopy in a rat perforator flap model. Plastic and Reconstructive Surgery 2020, 146(5), 1044-105

70Hummelink S, Kruit AS, van Vlaenderen ARW, Schreinemachers MJM, Steenbergen W, Ulrich DJO. Post-operative monitoring of free flaps using a low-cost thermal camera: a pilot study. European Journal of Plastic Surgery 2020; 43 (5): 589-596.

71.Sokol KK, Black GE, Willey SB, Kniery K, Marko ST, Eckert MJ, Martin MJ. There's an app for that: A handheld smartphone-based infrared imaging device to assess adequacy and level of aortic occlusion during REBOA. Journal of Trauma and Acute Care Surgery 2017; 82 (1): 102-108.

72.Barron MR, Kuckelman JP, McClellan JM, Derickson MJ, Phillips CJ, Marko ST, Smith JP, Eckert MJ, Martin MJ. Smartphone-based mobile thermal imaging technology to assess limb perfusion and tourniquet effectiveness under normal and blackout conditions. Journal of Trauma and Acute Care Surgery 2017; 83 (6): 1129-1135

73.Pereira CB, Kunczik J, Bleich A, Haeger C, Kiessling F, Thum T, Tolba R, Lindauer U, Treue S, Czaplik M. Perspective review of optical imaging in welfare assessment in animal-based research. Journal of Biomedical Optics 2019; 24 (7): 056109.

74.Lin SD, Chen K, Chen W. Thermal Face Recognition Based on Physiological Information. Proceedings - International Conference on Image Processing ICIP. 2019; 8803688: pp, 3497-3501

75.O'Kane BL, Crenshaw MD, D'Agostino J, Tomkinson D. Human target detection using thermal systems. Proceedings of SPIE - The International Society for Optical Engineering 1992; 2075: 75-88.

76.Yoshikawa H, Uchiyama A, Nishikawa Y, Higashino T. Poster: Combining a thermal camera and a wristband sensor for thermal comfort estimation. Proceedings of the 2019 ACM International Joint Conference on Pervasive and Ubiquitous Computing and Proceedings of the 2019 ACM International Symposium on Wearable Computers 2019; pp, 238-241.

77.Kim W, Lee S, Kim S, Jo S, Yoo C, Hwang I, Kang S, Song J. Dyadic Mirror: Everyday Second-person Live-view for Empathetic Reflection upon Parent-child Interaction. Proceedings of the ACM on Interactive Mobile Wearable and Ubiquitous Technologies 2020; 4 (3): 86.

78.Kirimtat A, Krejcar O, Selamat A, Herrera-Viedma E. FLIR vs SEEK thermal cameras in biomedicine: Comparative diagnosis through infrared thermography. BMC Bioinformatics 2020; 21: 88 .

79.Kirimtat A, Krejcar O. FLIR vs SEEK in Biomedical Applications of Infrared Thermography.; Lecture Notes in Computer Science; 2018, 10814: 221-230.

80.Ammer K. Medical Thermology 2017 - A computer-assisted literature survey. Thermology International 2018; 28 (3): 139-178.

81.Ammer K. Medical Thermology 2019 - a computer-assisted literature survey. Thermology International 2020; 30 (1): 7-36.

82.Ammer K. Should we perpetuate misconceptions of the past? Thermology International 2020; 30 (2): 47-50.

83.Aubakir B, Nurimbetov B, Tursynbek I, Varol HA. Vital sign monitoring utilizing Eulerian video magnification and thermography. 2016; Proceedings of the Annual International Conference of the IEEE Engineering in Medicine and Biology Society EMBS 2016; 59148: pp. 3527-3530.

84.Brown GDS, Latonio CEA, Oanes RDN, Valentin KR, Zara EJF, Serrano KKD, Guevara EC, Dela Cruz AR, Bandala AA, Vicerra RRP. Machine vision for rat detection using thermal and visual information. HNICEM 2017 - 9th International Conference on Humanoid Nanotechnology Information Technology Communication and Control Environment and Management 2018: 1-6.

85.Cândido MGL, Tinôco IDFF, Herker LP, Ireno TFP, Andrade RR, Gates RS. Evaluation of a low-cost thermographic camera for poultry temperature. 10th International Livestock Environment Symposium ILES 2018-143.

86.Haukebø T, Steinkjer J, Finlayson B. Infrared Imagery and Inert Media Used in Treating Upwelling Groundwater with Rotenone. North American Journal of Fisheries Management 2018; 38 (6): 1299-1305.

87.Daffara C, Muradore R, Piccinelli N, Gaburro N, de Rubeis T, Ambrosini D. A cost-effective system for aerial 3d thermography of buildings. Journal of Imaging 2020; 6 (8) art.no. 76.

88.Hodges RJ. Seeing the heat with inexpensive thermography: Natural history observations on the northern viper (Vipera berus) and grass snake (Natrix Helvetica). Herpetological Bulletin 2018; (144): 5-13.

89.Unger SD, Rollins MA, Thompson CM. Hot- or Cold-Blooded? A Laboratory Activity that Uses Accessible Techno- logy to Investigate Thermoregulation in Animals. American Biology Teacher 2020; 82 (4): 227-233.

90.Khalili Moghaddam G, Lowe CR. Ex vivo biosignatures. SpringerBriefs in Applied Sciences and Technology 2019; pp. 51-104.

91.García-Tejero IF, Ortega-Arévalo CJ, Iglesias-Contreras M, Moreno JM, Souza L, Tavira SC, Durán-Zuazo VH. Assessing the crop-water status in almond (Prunus dulcis mill.) trees via thermal imaging camera connected to smartphone. Sensors 2018; 18 (4): 1050.

92.Naik S, Patel B. Thermal imaging with fuzzy classifier for maturity and size based non-destructive mango (Mangifera Indica L) grading. 2017 International Conference on Emerging Trends and Innovation in ICT ICEI 2017; art, no, 7977003: 15-20.

93.Takács S, Pék Z, Biró T, Helyes L. Heat stress detection in tomato under different irrigation treatments. Acta Horticulturae 2019; 1233: 47-52

94.Putra RA, Akbar LA, Hatmojo RBD, Mulyasih H, Nugroho YS. Smoldering combustion spread on a thin layer of Papuan peat. 2020; AIP Conference Proceedings 2255 art, no, 0700071

95.Petrie PR, Wang Y, Liu S, Lam S, Whitty MA, Skewes MA. The accuracy and utility of a low-cost thermal camera and smartphone-based system to assess grapevine water status. Biosystems Engineering 2019; 179: 126-139

96.Vera Zambrano M, Dutta B, Mercer DG, MacLean HL, Touchie MF. Assessment of moisture content measurement methods of dried food products in small-scale operations in developing countries: A review. Trends in Food Science and Technology 2019; 88: 484-496.

97.Ahlberg J. Visualization techniques for surveillance: Visualizing what cannot be seen and hiding what should not be seen. Konsthistorisk Tidskrift 2015; 84 (2): 123-138.

98.Martínez-Garrido MI, Fort R, Gómez-Heras M, Valles-Iriso J, Varas-Muriel MJ. A comprehensive study for moisture control in cultural heritage using non-destructive techniques. Journal of Applied Geophysics 2018; 155: 36-52.

99.Tsay R-J. A Study for Thermal Sensing Applied to Structural Leaking and Crack Estimation Application2019 IEEE Eurasia Conference on IOT Communication and Engineering ECICE 2019; 8942772: 526-529

100.Dib J, Sirlantzis K, Howells G. A Review on Negative Road Anomaly Detection Methods. IEEE Access 2020; 8: 57298-57316.

101.Du W, Zhao Y, Roy R, Addepalli S, Tinsley L. A review of miniaturised Non-Destructive Testing technologies for in-situ inspections. Procedia Manufacturing 2018; 16: 16-23.

102.Sahin CD, Pinar Mengüç M. Image registration method for mobile-device-based multispectral optical diagnostics for buildings. Applied Optics 2019; 58 (26): 7165-7173.

103.El Ammari K, Hammad A. Remote interactive collaboration in facilities management using BIM-based mixed reality. Automation in Construction 107 2019; art.no. 102940..

104.Fu T, Stipancic J, Miranda-Moreno L, Zangenehpour S, Synergies B, Saunier N. Traffic data collection using thermal camera under varying lighting and temperature conditions in multimodal environments. 2016 Transportation Association of Canada's Conference and Exhibition TAC 2016.

105.Fu T, Stipancic J, Zangenehpour S, Miranda-Moreno L, Saunier N. Automatic traffic data collection under varying lighting and temperature conditions in multimodal environments:

Thermal versus visible spectrum video-based systems. Journal of Advanced Transportation 2017; art, no, 5142732.

106.Nam Y, Nam Y-C. Vehicle classification based on images from visible light and thermal cameras. Eurasip Journal on Image and Video Processing 2018; 2018 (1): 5.

107.Janveja I, Nambi A, Bannur S, Gupta S, Padmanabhan V. InSight: Monitoring the State of the Driver in Low-Light Using Smartphones. Proceedings of the ACM on Interactive Mobile Wearable and Ubiquitous Technologies 2020; 4(3): 83.

108.Todorovici L, Bogdan R. Studying thermal behavior of buildings and vehicles by means of a mobile thermographic system. 24th Telecommunications Forum TELFOR 2016, 2017; art.no. 7818909.

109.Weber Y, Kanarachos S. CUPAC - The Coventry University public road dataset for automated cars. Data in Brief 2020; 28: 104950

110.Qiu C, Zhou Q, Wang D, Lou X, Li B. A study on the FLIR ONE PRO-based fault detection of communication control system. Proceedings - 2020 12th International Conference on Measuring Technology and Mechatronics Automation ICMTMA 2020; 9050202: 407-410.

111.El-Din DM, Hassanien AE, Hassanein EE. MSFMT: Multispectral fusion system based on deep transfer learning and Dempster-Shafer theory. Journal of Theoretical and Applied Information Technology 2020; 98 (6): 1037-1049.

112.Hadidi R, Cao J, Xie Y, Asgari B, Krishna T, Kim H. Characterizing the Deployment of Deep Neural Networks on Commercial Edge Devices. Proceedings of the 2019 IEEE International Symposium on Workload Characterization IISWC 2019; pp.35-48.

113.Hadidi R, Asgari B, Mudassar BA, Mukhopadhyay S, Yalamanchili S, Kim H. Demystifying the characteristics of 3D-stacked memories: A case study for Hybrid Memory Cube. Proceedings of the 2017 IEEE International Symposium on Workload Characterization IISWC 2017: 66-75.

114.Hayes AE, Montagna R, Finlayson GD. New applications of Spectral Edge image fusion. Proceedings of SPIE - The International Society for Optical Engineering 2016; 984009.

115.Imran M, O'Nils M, Kardeby V, Munir H. Demo: STC-CAM1 IR-visual based smart camera system. ACM International Conference Proceeding Series 2015; pp, 195-196.

116.Inostroza F, Cardenas J, Godoy SE, Figueroa M. Embedded Multimodal Registration of Visible Images on Long-Wave Infrared Video in Real Time. Proceedings - 19th Euromicro Conference on Digital System Design DSD 2016 2016; 7723551: 176-183.

117.Kang S, Choi H, Park S, Park C, Lee J, Lee U, Lee S-J. Fire in your hands: Understanding thermal behavior of smartphones. Proceedings of the Annual International Conference on Mobile Computing and Networking MOBICOM, 2019.

118.Kenny C, Liboiron M, Wylie SA. Seeing power with a flashlight: DIY thermal sensing technology in the classroom. Social Studies of Science 2019; 49 (1): 3-28.

119.Klaessens JH, Van Der Veen A, Verdaasdonk RM. Comparison of the temperature accuracy between smart phone based and high-end thermal cameras using a temperature gradient phantom. Progress in Biomedical Optics and Imaging - Proceedings of SPIE 2017; art. no. 100560D.

120.Yoshikawa H, Uchiyama A, Higashino T. Dynamic Offset Correction for Smartphone Thermal Cameras Using a Wristband Sensor. 2019 IEEE International Conference on Pervasive Computing and Communications Workshops PerCom Workshops 2019; 8730732: 65-170.

121.Yoshikawa H, Uchiyama A, Higashino T. Thermalwrist: Smartphone thermal camera correction using a wristband sensor†. Sensors 2019; 19 (18): 3826.

122.Kluwe B, Christian D, Miknis M, Plassmann P, Jones C. Segmentation of infrared images using stereophotogrammetry. Lecture Notes in Computational Vision and Biomechanics 2018; 27: 1025-1034.

123.Kniaz VV, Mizginov VA. Thermal texture generation and 3D model reconstruction using SFM and GAN. International Archives of the Photogrammetry Remote Sensing and Spatial Information Sciences - ISPRS Archives 2018; 42 (2): 519-524.

124.Link T, Baraba M. Low cost 3D-depth and thermal sensor trends and applications. Energieautarke Sensorik - Beitrage des 7, GMM-Workshops 2014; pp, 81-85.

125.Zhou J, Guo Y, Shinde S, Hosseinbeig A, Patnaik A, Izadi OH, Zeng C, Shi J, Maeshima J, Shumiya H, Araki K, Pommerenke DJ. Measurement Techniques to Identify Soft Failure Sensitivity to ESD. IEEE Transactions on Electromagnetic Compatibility 2020; 62 (4):1007-1016.

126.López-Medina MÁ, Espinilla M, Nugent C, Quero JM. Evaluation of convolutional neural networks for the classification of falls from heterogeneous thermal vision sensors International Journal of Distributed Sensor Networks. 2020; 16 (5)

127.Luo C, Goncalves J, Velloso E, Kostakos V. A survey of context simulation for testing mobile context-aware applications. ACM Computing Surveys 2020; 53 (1): 21.

128.Lynch CN, Devaney N, Drimbarean A. Computational methods for improving thermal imaging for consumer devices. Proceedings of SPIE - The International Society for Optical Engineering 2015; art.no. 94850P.

129.Malmivirta T, Hamberg J, Lagerspetz E, Li X, Peltonen E, Flores H, Nurmi P. Hot or not? robust and accurate continuous thermal imaging on FLIR cameras. 2019 IEEE International Conference on Pervasive Computing and Communications PerCom 2019; art, no, 8767423.

130.Mauriello ML, McNally B, Buntain C, Bagalkotkar S, Kushnir S, Froehlich JE. A large-scale analysis of YouTube videos depicting everyday thermal camera use. MobileHCI 2018 - Beyond Mobile: The Next 20 Years - 20th International Conference on Human-Computer Interaction with Mobile Devices and Services Conference Proceedings 2018; art, no, a37.

131.Mauriello ML, McNally B, Froehlich JE. Thermporal: An easy-to-deploy temporal thermographic sensor system to support residential energy audits. Conference on Human Factors in Computing Systems - Proceedings, 2019;

132.Mauriello ML, Saha M, Brown E, Froehlich JE. Exploring novice approaches to smartphone-based thermographic energy auditing: A field study. Conference on Human Factors in Computing Systems - Proceedings 2017; pp, 1768-1780.

133.McKeown M, Lavrov A, Shahrad M, Jackson PJ, Fu Y, Balkind J, Nguyen TM, Lim K, Zhou Y, Wentzlaff D. Power and Energy Characterization of an Open Source 25-Core Manycore Processor. Proceedings - International Symposium on High-Performance Computer Architecture 2018; pp, 762-775.

134.Mosenia A, Jha NK. OpSecure: A secure unidirectional optical channel for implantable medical devices. IEEE Transactions on Multi-Scale Computing Systems 2018; 4 (3): 410-419..

135.Palmerius KL, Schönborn K. Visualization of heat transfer using projector-based spatial augmented reality. Lecture Notes in Computer Science (including subseries Lecture Notes in Artificial Intelligence and Lecture Notes in Bioinformatics 2016; 9768: 407-417.

136.Pittaluga F, Zivkovic A, Koppal SJ. Sensor-level privacy for thermal cameras. Proceedings of 2016 IEEE International Conference on Computational Photography (ICCP) 2016, art, no, 7492877.

137.Ryseck P, Yeo D, Hrishikeshavan V, Chopra I. Expanding the mission capabilities of a quadrotor biplane tail-sitter with morphing winglets. AIAA Scitech 2020; Forum 1 PartF.

138.Salmon PC, Meissner PL. Mobile bot swarms: They're closer than you might think! IEEE Consumer Electronics Magazine 2015; 4 (1): 58-65.

139.Schönborn K, Haglund J, Xie C. Pupils' early explorations of thermoimaging to interpret heat and temperature. Journal of Baltic Science Education 2014; 13 (1): 118-132.

Address for Correspondence

Prof Dr med Kurt Ammer PhD
European Association of Thermology
1170 Vienna, Austria
email: kammer1950@aol.com

Sonography and Thermography in the Painful Shoulder Syndrome

Review of the book "Sonografické a Termografické Nalezy Ramena" by Jozef Gabrhel
(Vzdelávcie centrum SLK, 2020, ISBN 978-80-88320-39-5)

Kurt Ammer

Editor in chief, Thermology international, European Association of Thermology, Vienna, Austria

The long lasting EAT member Dr Jozef Gabrhel published a comprehensive case book on shoulder pain. Although the book is written in Slovak language which should be reasonable understood by Czech or Polish thermologists, this case collection is of interest for all who are interested in thermal imaging irrespective to their natural language.

As in his previous articles on pain syndromes located at the knee, the low back or the elbow, the author combines thermal imaging and sonography for the evaluation of the patients' complaints. Intended as course book for continuous medical education organised by the Slovak Chamber of Physicians, this publication displays on 149 pages with 225 thermal and 310 sonographic images the abundance of Dr Gabrhel's experience in applying either imaging technique in painful conditions of the shoulder region.

The book is organised in ten sections, starting with 1.) bony defects in the humerus head, 2.) lesions in various bursae and recessus 3.) tendon lesions of the biceps brachii muscle 4.) findings at the acromioclavicular joint 5.) lesions of the subscapularis muscle 6.) lesions of the supraspinatus muscle, 7.) lesions of the infraspinatus and teres minor muscle 8.) ruptures of the major pectoral muscle, the triceps, the deltoid and rhomboid muscles 9.) bony fractures and 10.) osteosynthesis. In the beginning ofeach section the anatomy is sketched, and normal thermographic and sonographic findings are provided. They are followed by combined findings in thermal imaging and sonography, occasionally supplemented by radiographs or magnetic resonance images.

This case collection clearly demonstrate that similar structural lesions are not always associated with the same pattern of skin temperature distribution, underlining the complimentary information obtained by either imaging techniques. Since the shoulder is regarded as the most complex joint of the locomotor apparatus, it is not unexpected that a wide range of lesions can be detected by a carefully evaluation with combined imaging modalities as Dr Gabrhel demonstrated with this book. As the preface of this book mentioned, that other books of this kind are planned, I look with curiosity forward to see them, preferably in an bilingual version (Slovak and English).

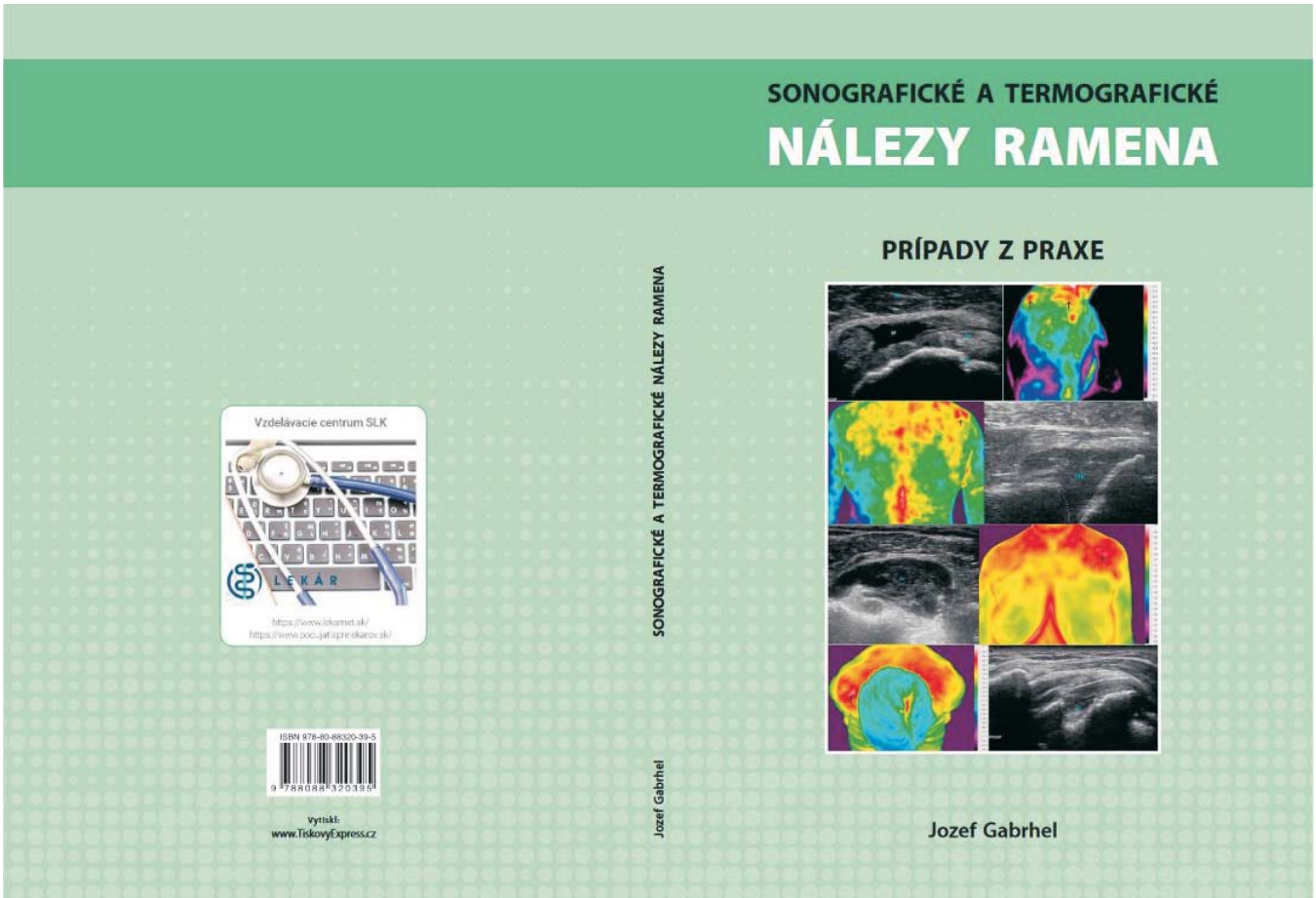

Letter to the Editor

Missed reference in the article published in Thermology international 2020; 30(3) 89-90

Dear Editor,

Following on from my review in the last issue of Thermology International [1] of the paper by Maley et. al. [2], I was delighted to receive a message from EAT member Prof. George Havenith at the Environmental Ergonomics Research Centre, Loughborough University, UK.

Prof. Havenith drew to my attention his recent article in the Journal of Thermal Biology, authored with his colleague Alex Lloyd [3] which also reviews the Maley et. al. paper and offers some further very interesting criticisms of the study.

In a year when the opportunity to discuss research "face-to-face" has been severely limited, it is good to see that EAT members remain at the forefront of scientific debate in the field of biomedical temperature measurement by means of their contribution to journals.

I hope that we can all meet again to expand on our debates as soon as possible in 2021.

Regards

Kevin J. Howell PhD ASIS FRPS
Institute of Immnunity and Transplantation,
Royal Free Hospital, London, UK
President, European Association of Thermology

References.

1.Howell KJ. Care required in comparing thermographic methods to other thermological techniques Thermol.Int. 2020; 30: 89-90

2.Maley MJ, Hunt AP, Bach AJE, Eglin CM, Costello JT. Infrared cameras overestimate skin temperature during rewarming from cold exposure. J. Therm. Biol. 2020;91:102614

3.Havenith G, Lloyd AB. Counterpoint to „Infrared cameras overestimate skin temperature during rewarming from cold exposure." J. Therm. Biol. 2020;92:102663

Meetings

Due to the on-going Covid-19 pandemy, we have not received any reliable information on Thermology conferences planned for the next 6 months.

There might be small opportunity for the traditional meeting in Zakopane, but propably not prior to the end of April or in early May.

The date for EAT2021 conference in Wroclaw seems to be save, however, the EAT Board and the Conference Organising Committee will discuss that matter in due course in a video conference.

CALL FOR ABSTRACTS

WROCŁAW UNIVERSITY OF ENVIRONMENTAL AND LIFE SCIENCES

XV Congress of the European Association of Thermology

1st – 4th September 2021

Faculty of Biology and Animal Science

Wrocław University of Environmental and Life Sciences

Wrocław, Poland

XV Congress of the European Association of Thermology

Wrocław • POLAND 2021

Supported by: Thermetrix Limited

Making Life Better

www.eurothermology.org/XVCongress.html

The EAT and Wrocław University of Environmental and Life Sciences are delighted to invite you to participate in the XV EAT Congress in Wrocław, Poland from 1st to 4th September 2021.

The European Association of Thermology exists to promote, support and disseminate research in thermometry and thermal imaging in the fields of human and veterinary medicine and biology. We do this through our peer-reviewed journal Thermology International, regional seminars around Europe, and our flagship Congress, which takes place every three years.

Following on from the most recent meetings in Porto (2012), Madrid (2015) and London (2018) the Congress heads to eastern Europe for 2021 to Wrocław in Poland.

The Organising Committee looks forward to welcoming you to Wrocław University of Environmental and Life Sciences in the summer of 2021.

Dr. Kevin Howell
EAT President

VENUE.

Wroclaw lies on the banks of the River Oder in western Poland, and is the capital of the Lower Silesian Vovoideship. It was the European Capital of Culture in 2016, and won the "European Best Destination" title in 2018.

Our venue will be the Faculty of Biology and Animal Science at the prestigious University of Environmental and Life Sciences on Chelmonskiego Street in the eastern suburbs of Wrocław. The Faculty building boasts excellent conference facilities including a large lecture theatre, ample lobby space for networking and poster presentations, and a spacious restaurant for lunch breaks. This is the perfect environment for delegates to present their thermological research at Europe's flagship biomedical temperature congress.

ORGANISING COMMITTEE	INTERNATIONAL SCIENTIFIC COMMITTEE
Maria Soroko (POL), Chair	**Kurt Ammer (AUT), Chair**
Kurt Ammer (AUT)	John Allen (GBR)
Wanda Górniak (POL)	Danilo Gomes Moreira (BRA)
Kevin Howell (GBR)	Kevin Howell (GBR)
Anna Jung (POL)	Anna Jung (POL)
Damian Knecht (POL)	Mariusz Korczyński (POL)
Alicja Kowalczyk (POL)	Robert Kupczyński (POL)
Sebastian Opaliński (POL)	James Mercer (NOR)
Adam Roman (POL)	Sebastian Opaliński (POL)
Adérito Seixas (POR)	David Pascoe (USA)
Manuel Sillero-Quintana (ESP)	Adérito Seixas (POR)
Ricardo Vardasca (POR)	Manuel Sillero-Quintana (ESP)
Klaudia Wlaźlak (POL)	Maria Soroko (POL)
Anna Zielak-Steciwko (POL)	Hisashi Usuki (JPN)
	Ricardo Vardasca (POR)
	Ho Yeol Zhang (KOR)

KEY DATES.

Abstract submission will open online on 31st August 2020, and authors will be notified of acceptance for oral or poster presentation by 1st March 2021.

31st August 2020. Opening of abstract submission and registration.
31st December 2020. Abstract submission deadline.
1st March 2021. Acceptance notification to authors.
3rd May 2021. End of Early Registration and deadline for registration of presenting authors

XV Congress of the European Association of Thermology
Wrocław · POLAND 2021

XV EAT CONGRESS, 1st – 4th September 2021, Wrocław.

REGISTRATION FEES (*)

	Early Registration (Until 03 MAY 2021)	Late Registration (After 03 MAY 2021)
EAT MEMBER	€250	€300
Non-Member	€300	€350
One-day registration	€100	€150
Student	€100	€150
Accompanying person	€50	€50

(*) Further information about the registration process is online at www.eurothermology.org/XVCongress.html Registration includes access to all congress sessions, congress lunch and coffee breaks, the Gala Dinner, and other congress social programme events.

ACCOMMODATION

Recommended hotels:

1. **Hotel ZOO**

Address: ul. Wroblewskiego 7, 51-627 Wroclaw
website: http://zoo-hotel.pl/

2. **Radisson Blu Hotel Wroclaw*****

Address: ul. Purkyniego 10, 50-156 Wroclaw
website: https://www.radissonblu.com/pl/hotel-wroclaw

3. **Grape Hotel & Restaurant*****

Address: Parkowa 8, 51-616 Wroclaw
website: https://www.grapehotel.pl

4. **URO Wroclaw Old Town*****

Address: Pawła Włodkowica 6, 50-072 Wroclaw
website: https://purohotel.pl/pl/wroclaw

5. **HOTEL EUROPEUM *****

Address: ul. Kazimierza Wielkiego 27A, 50-077 Wroclaw
website: https://europeum.pl

6. **Hotel Mercure Wroclaw Centrum******

Address: pl. Dominikański 1, 50-159, Wroclaw
website: https://www.accorhotels.com/pl/hotel-3374-hotel-mercure-wroclaw-centrum/index.shtml

ACCOMPANYING PERSONS

All accompanying persons will be invited to join the Congress Gala Dinner and full social programme upon payment of the appropriate €50 fee.

KEY MEETING THEMES

- Infrared thermography in biomedicine.
- Temperature measurement in animal welfare, veterinary applications and equine physiology.
- Contact temperature measurement.
- Hardware and software solutions for infrared imaging.
- Biomedical applications: surgery, neurology, vascular and pain syndromes.
- Thermometry in exercise physiology, rehabilitation, and human performance research.
- Calibration and traceability in biomedical thermometry.

ABOUT WROCŁAW

Wrocław is also called "The Venice of the North" due to the fact that, after Amsterdam, Venice and St. Petersburg, it has the biggest number of bridges and footbridges in Europe.

Notable landmarks include the 10th century Cathedral, the Centennial Hall from 1913 (one of the UNESCO world heritage sites), and the distinctive architecture of the Town Hall and Market Square. Wrocław is also host to the Racławice Panorama, a 114m-long cycloramic painting from 1894, commemorating the 100th anniversary of the Battle of Racławice. In recent years Wrocław has also become well-known for its "little people" or "dwarves": small figurines scattered across the city streets which were first conceived as part of the city's anti-communist movement in 2005. These now number more than 350, and can be located with the help of a dedicated tourist map. Wrocław Zoo, close to our congress venue, is the oldest zoo in Poland, and the third largest zoological gardens in the world in terms of the number of species on display. In summertime, large numbers of visitors are attracted at night to Wrocław's "Multimedia Fountain" close to the Centennial Hall. This is one of the largest operating fountains in Europe, and stages dramatic light shows set to music. We will have the opportunity to visit this spectacle as part of the congress social programme.

TRAVEL

COPERNICUS AIRPORT WROCŁAW is about 10 km from the city centre, and connects Wrocław with Warsaw, Gdansk, and destinations throughout Europe. From the airport you can reach the city centre by a shuttle bus (journey time about 30 minutes), or by bus No. 106, which leaves every 15 minutes (journey time about 40 minutes) or by taxi. Wrocław's main rail station, WROCŁAW GŁÓWNY, connects the city to other major destinations across Poland and eastern Europe. Wrocław's central bus station is located at 1/11 ul. Sucha, adjacent to the main railway station, and connects the city by road to all major Polish and European destinations.

Preliminary Schedule.

XV Congress of the European Association of Thermology, 1st – 4th September 2021, Wrocław University of Environmental and Life Sciences.

Time	Wednesday	Thursday	Friday	Saturday
8.30	Course Registration	Registration	Registration	Tour around Wrocław's Old Town and Ostrów Tumski 
9.00 - 10.30	Short Course on Medical Thermography	Morning session 1	Morning session 1	
10.30 - 11.00		Coffee break	Coffee break	
11.00 – 12.30		Morning session 2	Morning session 2	
12.30 – 13.00		Poster viewing 1	Poster viewing 2	
13.00 – 14.00		Lunch	Lunch	
14.00 – 15.30		Afternoon session 1	Afternoon session 1	
15.30- 16.15		Tea break	Tea break	
16.15 – 17.30		Afternoon session 2	Afternoon session 2	
17.30 – 18.30	Registration		EAT General Assembly	
18.30 – 20.00	Welcome Reception, Faculty of Biology and Animal Science			
19.00- 22.00		Gala Dinner at Summer Restaurant	Fountain show	

European Association of Thermology

Short Course on Medical Thermography

Wednesday 1st September 2021, Wrocław University of Environmental and Life Sciences Wrocław, Poland

Following on from successful courses in Porto, Madrid and London, the next EAT Short Course on Medical Thermography will take place immediately prior to the EAT 2021 Congress in Wrocław, Poland. The course aims to deliver a thorough introduction over one full teaching day to basic thermal physiology and the principles of infrared thermography for human body surface temperature measurement. It will be taught by an experienced faculty of EAT clinicians, biomedical researchers and imaging scientists. Aspects of reliable thermogram capture will be demonstrated in a laboratory session, and students will have the opportunity to practice thermal image analysis in a supervised "hands-on" session.

Syllabus

- Physical principles of heat transfer
- Principles of thermal physiology/skin blood perfusion
- Standardisation of thermal imaging, recording and analysis
- Quality assurance for thermal imaging systems
- Producing a thermographic report
- Provocation tests
- Image analysis
- Hands-on supervised practice
- Educational resources

Registration

The course fee (inclusive of lunch and coffee breaks) is €200
Register from 1st January 2021: details online at www.eurothermology.org/education.html
Questions? Contact the EAT at eurothermology@gmail.com

XV Congress of the European Association of Thermology
Wrocław - POLAND 2021

XV EAT CONGRESS, 1st – 4th September 2021, Wrocław.

The Thermal Human Body

A Practical Guide to Thermal Imaging

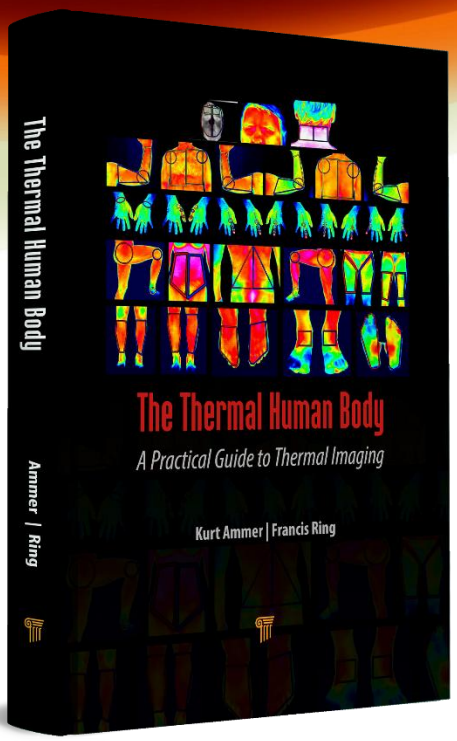

by
Kurt Ammer & Francis Ring

978-981-4745-82-6 (Hardback)
978-0-429-01998-2 (eBook)
US$149.95
260 Pages – 19 Color & 38 B/W Illustrations
May 2019

Key Features

- Combines the physics of heat transfer with thermal physiology to understand skin temperature distribution
- Provides a framework for standardized recording and analysis of medical thermal images
- Includes an atlas of body positions of proven reproducibility for infrared image capture
- Proposes regions of interests for reliable quantitative analysis

How to Order

SAVE 20% with FREE standard shipping when you order online at **www.crcpress.com** and enter Promo Code **PAN01.**
Alternatively, you can contact your nearest bookstore, or our distributor as follows:

CRC Press (*Taylor & Francis*)
6000 Broken Sound Parkway NW, Suite 300
Boca Raton, FL 33487, USA
Tel: +1 800-272-7737
Fax: +1 800-374-3401
Email: **orders@taylorandfrancis.com**

Reviews

"There is no way to study thermal imaging and not learn from the writings of Francis Ring and Kurt Ammer. Pioneers of the application of infrared thermography in medicine, the authors unveil the direction for a sensible use of the method. Luck for us—students, professionals and enthusiasts—because we can be grateful to receive a differentiated material that shortens the learning path. No doubt a remarkable book."
- **Prof. Danilo Gomes Moreira**, Science and Technology of Minas Gerais, Brazil

"This book is set to become essential reading for anyone who wants to perform reliable thermal imaging of the human body, whether it be in medicine, clinical practice, sports science or research."
- **Prof. Graham Machin**, National Physical Laboratory, UK

"This book is a wonderful practical guide that takes the reader through all the main stages required and will be of special interest for those interested in entering the fascinating field of clinical thermal imaging."
- **Prof. James B. Mercer**, UiT—The Arctic University of Norway, Norway

Description

This book is a guide for the constantly growing community of the users of medical thermal imaging. It describes where and how an infrared equipment can be used in a strictly standardized way and how one can ultimately comprehensively report the findings. Due to their insight into the complex mechanisms behind the distribution of surface temperature, future users of medical thermal imaging should be able to provide careful, and cautious, interpretations of infrared thermograms, thus avoiding the pitfalls of the past. The authors are well-known pioneers of the technique of infrared imaging in medicine who have combined strict standard-based evaluation of medical thermal images with their expertise in clinical medicine and related fields of health management.

JENNY STANFORD PUBLISHING